Métodos Sísmicos de Exploración

Exploración Petrolera - 2026

Frente de Onda: todos los puntos que son alcanzados por una onda simultáneamente

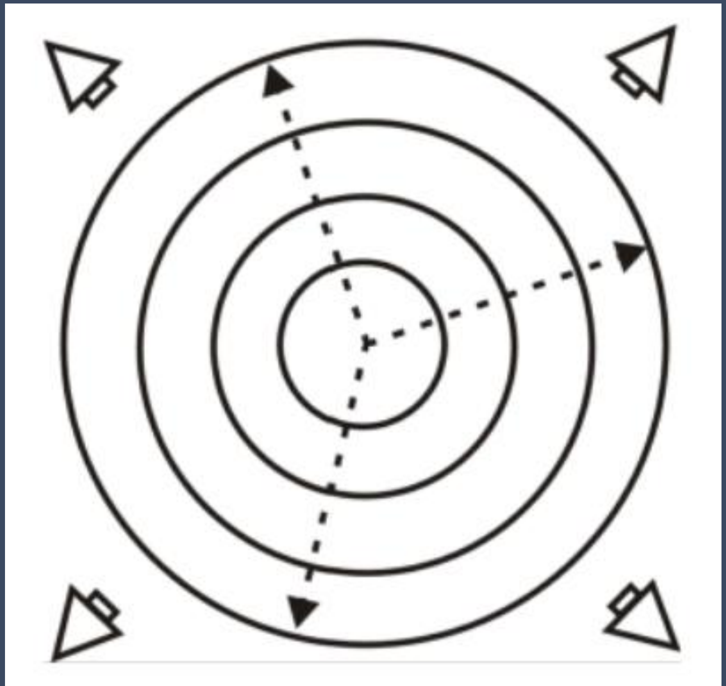

Ondas sinusoidales

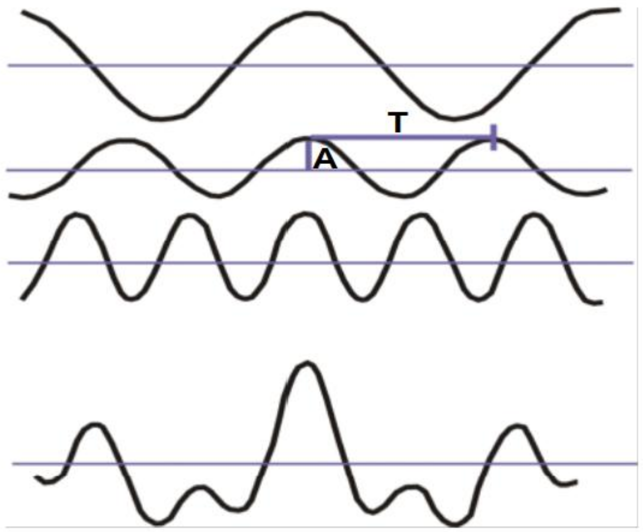

Figura N° 4. Ondas senoidales sumadas para obtener un pulso.

Ondícula

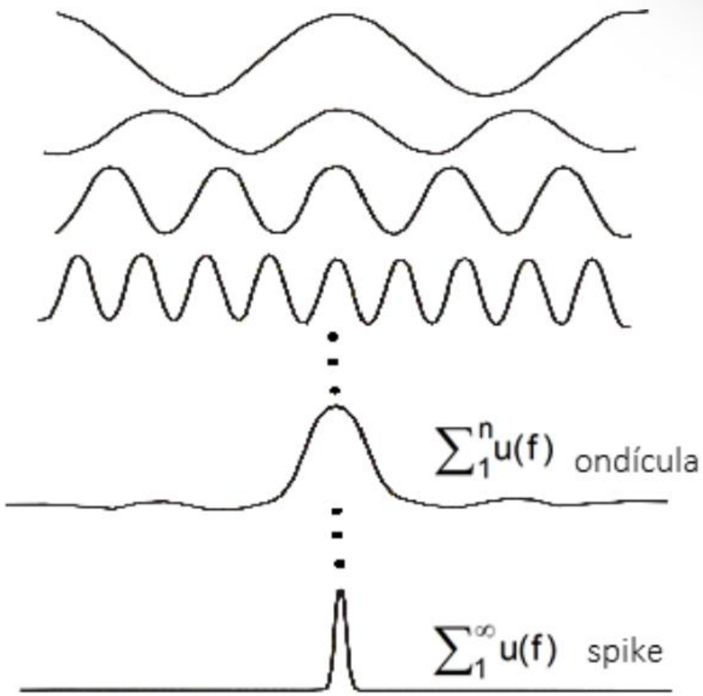

Ondas sísmicas: deformaciones que se propagan en el medio elástico que es la Tierra

Ondas P (primarias)
de presión

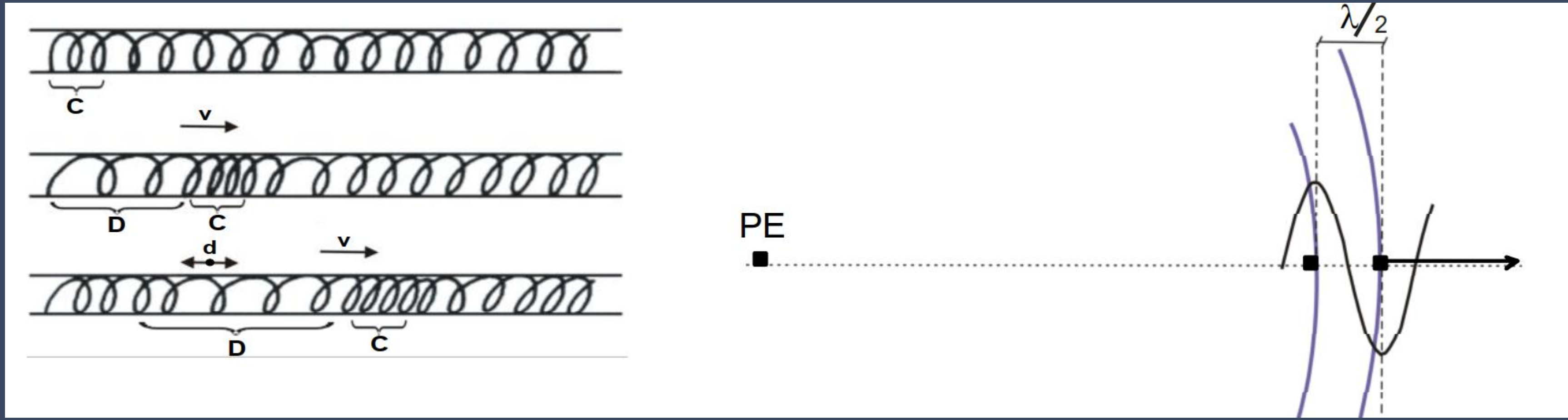

Ondas S (secundarias)
de cizalla

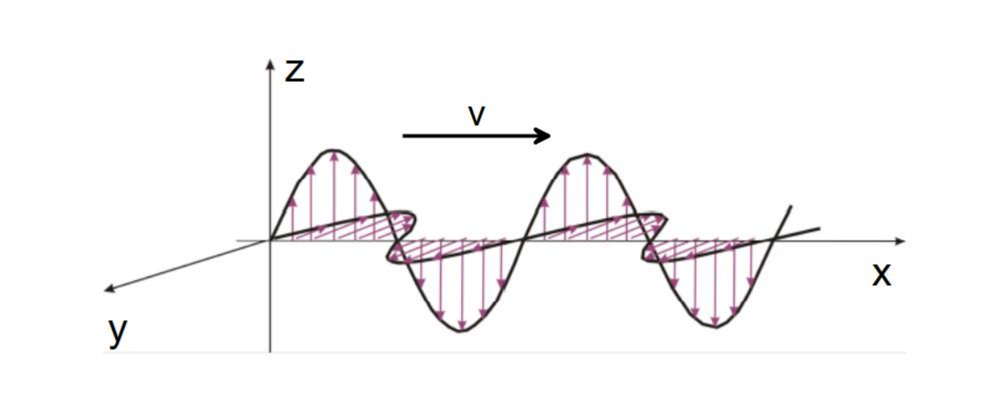

Ondas superficiales: Rayleigh y Love.

Velocidad de propagación

Ondas P > Ondas S > Ondas Superficiales

Principio de Huygens: Cada punto de un frente de ondas primarias se convierte en un nuevo foco de ondas elementales que avanza con la velocidad de la onda primaria y tienen la misma frecuencia.

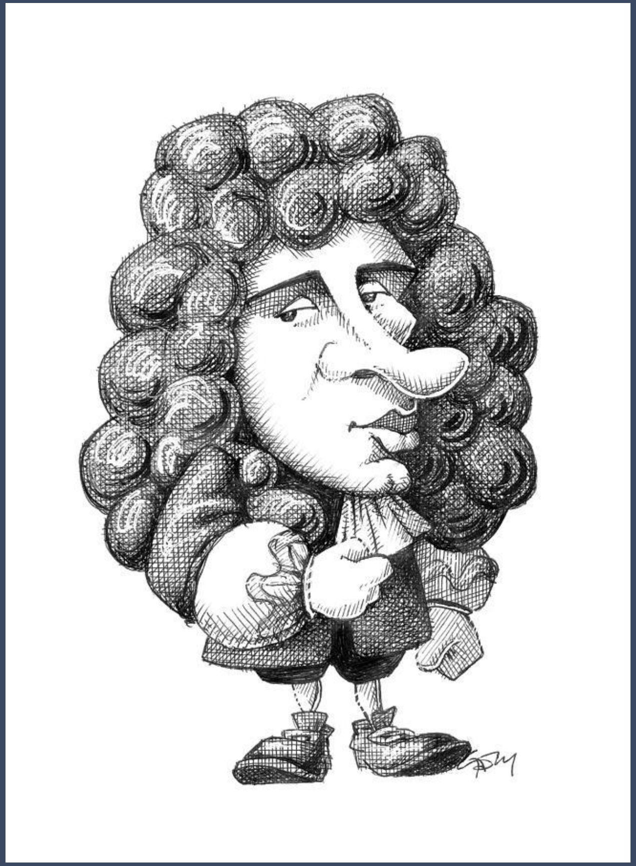

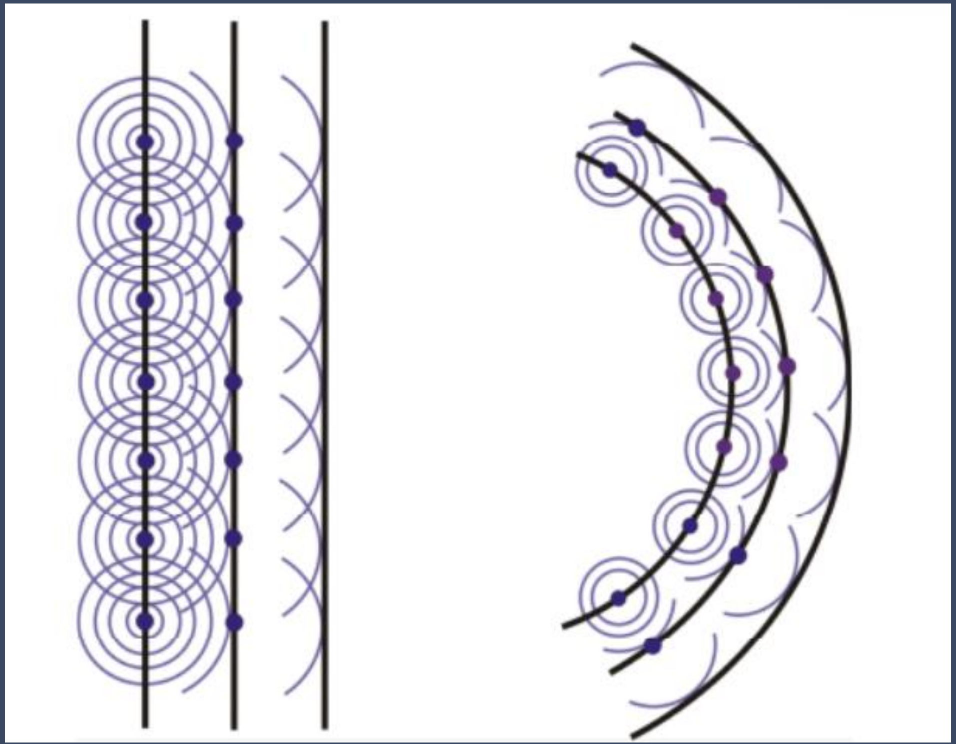

Pierre de Fermat (1662):
La propagación de un rayo sísmico entre un receptor y un emisor se produce a siguiendo un camino de tiempo mínimo

Willebrord Snel van Royen –
Snellius (1621)

Leyes de Snell – Descartes

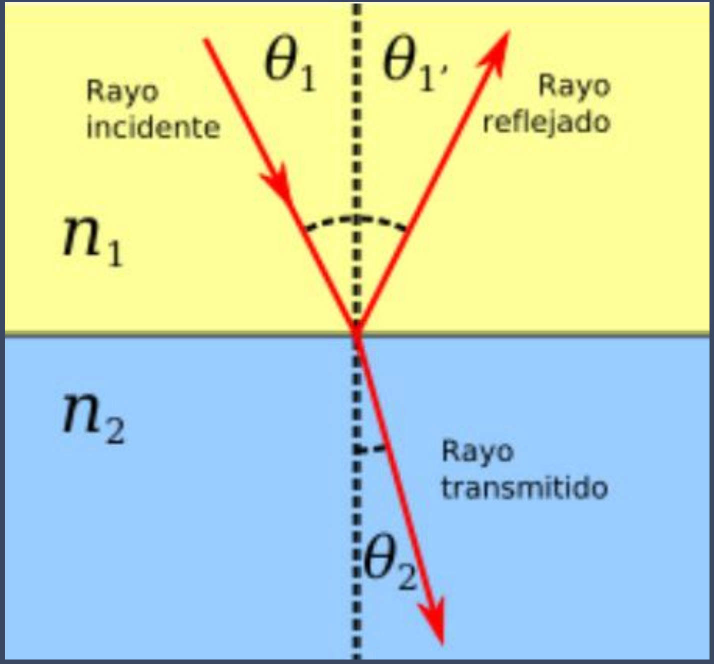

$$\frac{sen(\theta_1)}{sen(\theta_2)} = \frac{V_1}{V_2}$$

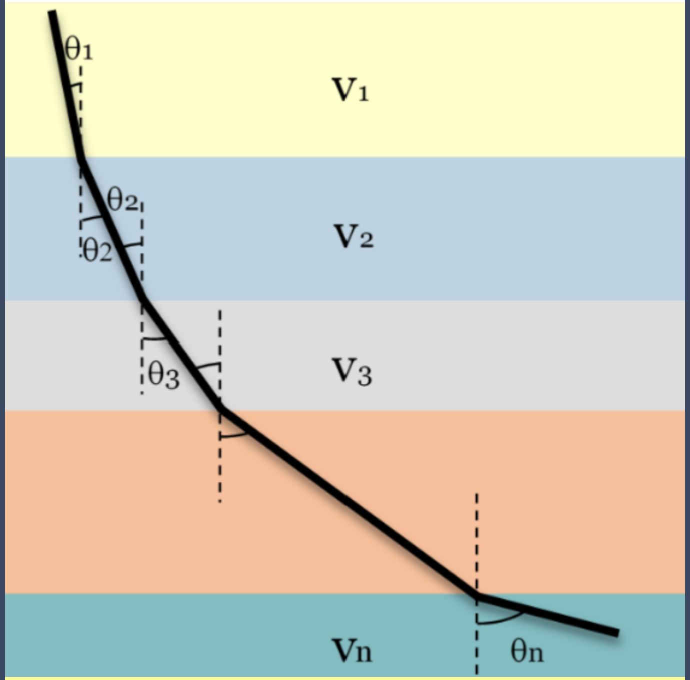

$$\frac{sen(\theta_1)}{sen(\theta_n)} = \frac{V_1}{V_n}$$

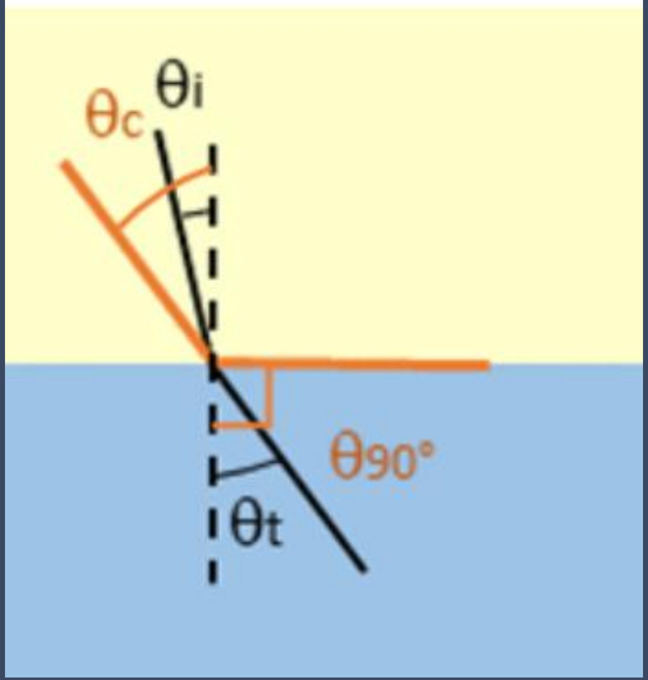

Impedancia Acústica

Resistencia que opone el medio a la propagación de una perturbación

$$Z = \rho \cdot V$$

Ígneas > Calizas > Lutitas > Arenisca porosas > Arenisca con gas

Coeficiente de reflexión

Proporción de energía incidente que se refleja

$$C_R = \frac{Z_2 - Z_1}{Z_2 + Z_1}$$

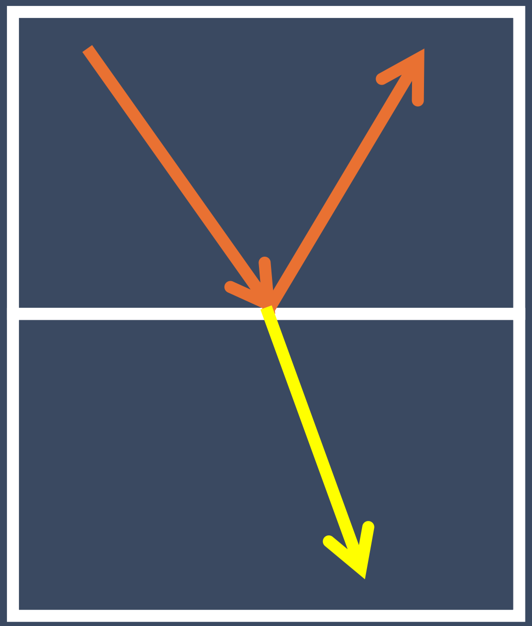

$$Z_1 = \rho_1 \cdot V_1$$

$$Z_2 = \rho_2 \cdot V_2$$

Instrumental

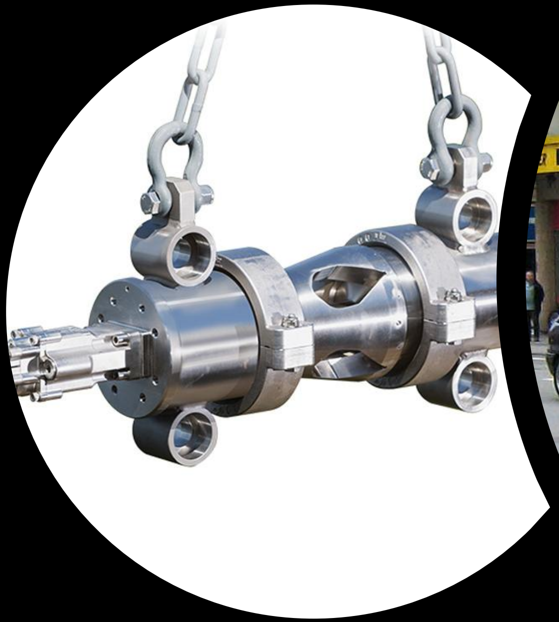

Air Gun

Vibroseis

Geófonos

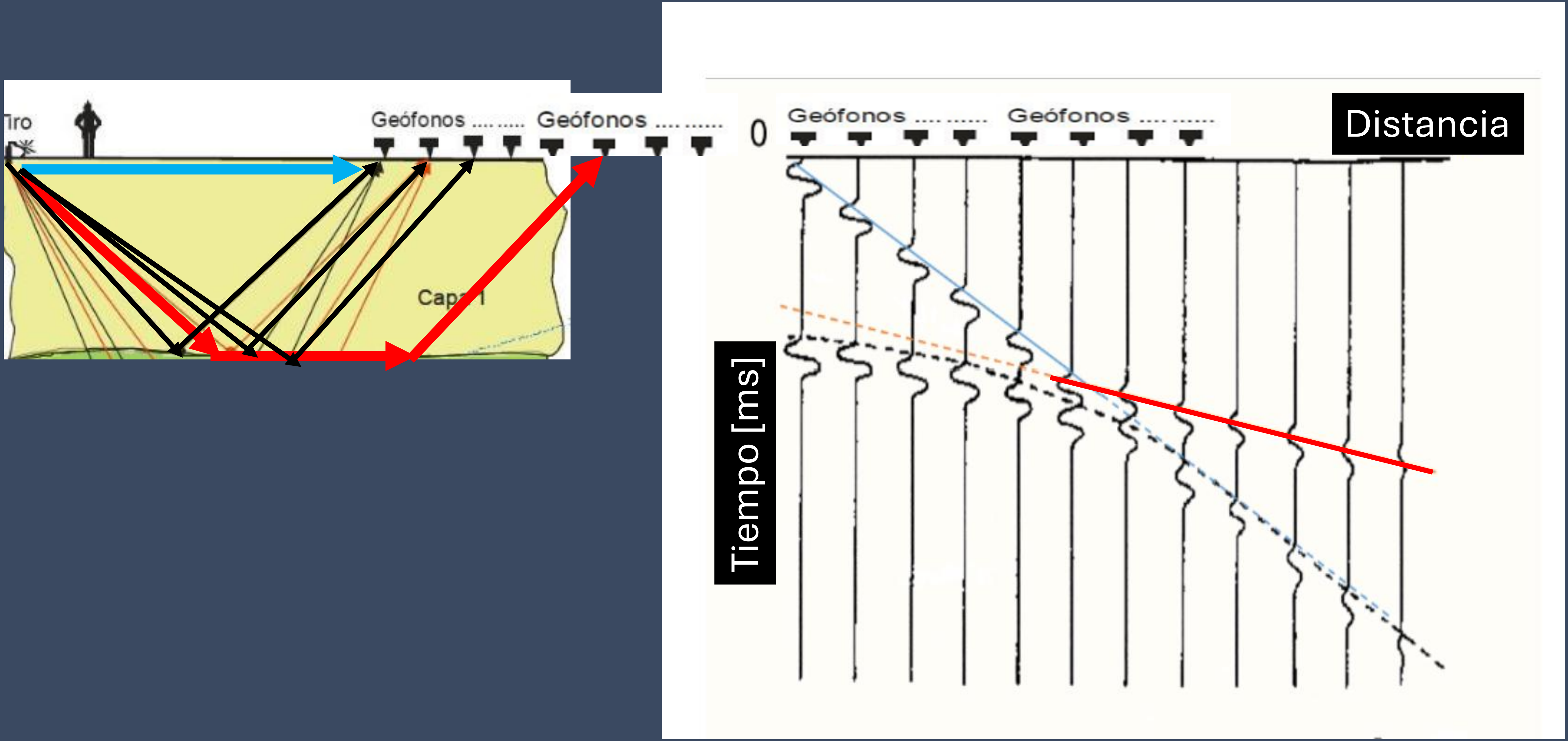
Tiro
Geófonos ....
Geófonos ....
0
Geófonos ....
Geófonos ....
Distancia
Tiempo [ms]

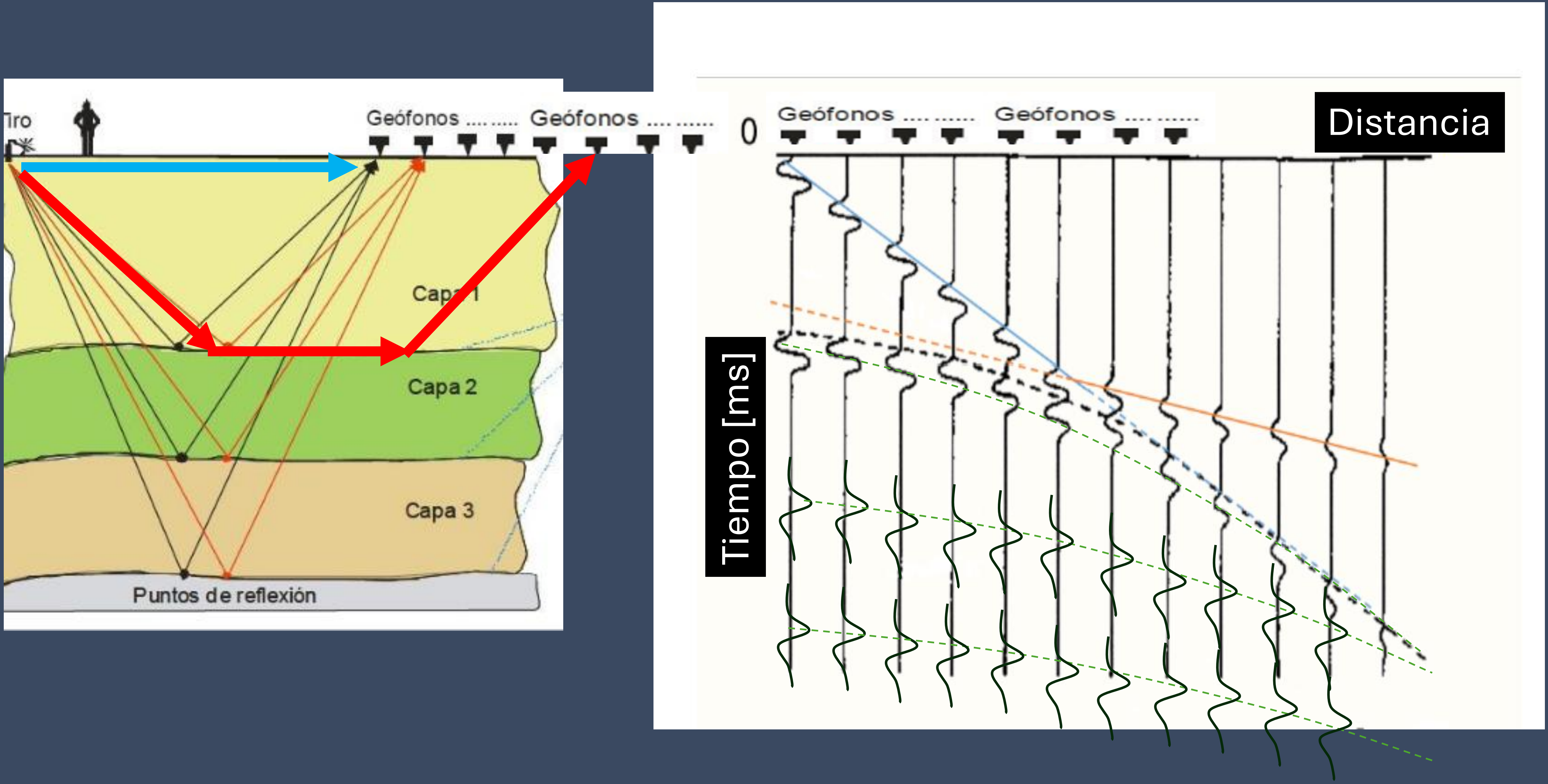

Tiro
Geófonos ....
Geófonos ....
Capa 1
Capa 2
Capa 3
Puntos de reflexión
0
Geófonos ....
Geófonos ....
Distancia
Tiempo [ms]

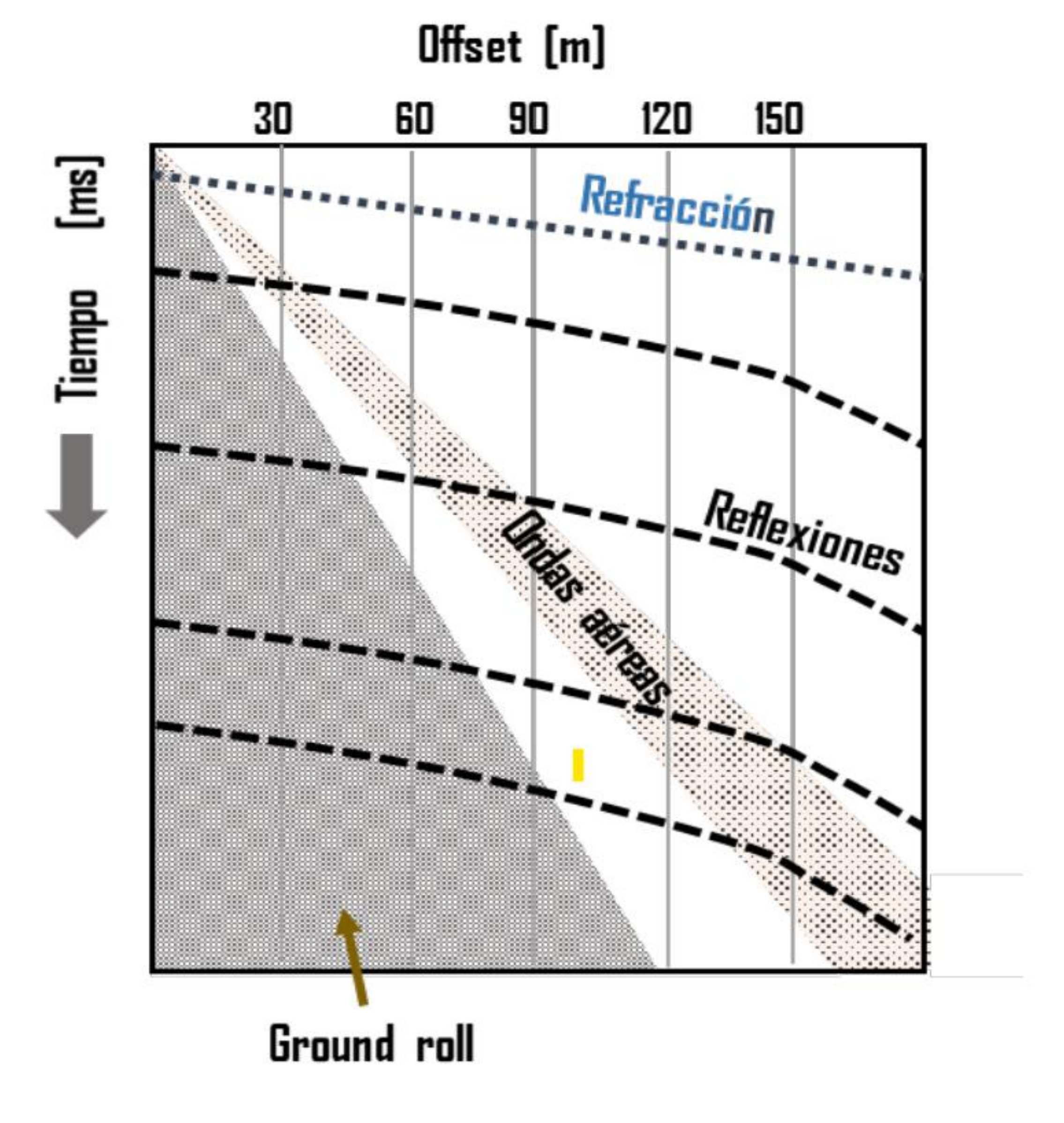
Offset [m]
30
60
90
120
150
Tiempo [ms]
Refracción
Reflexiones
Ondas aéreas
Ground roll

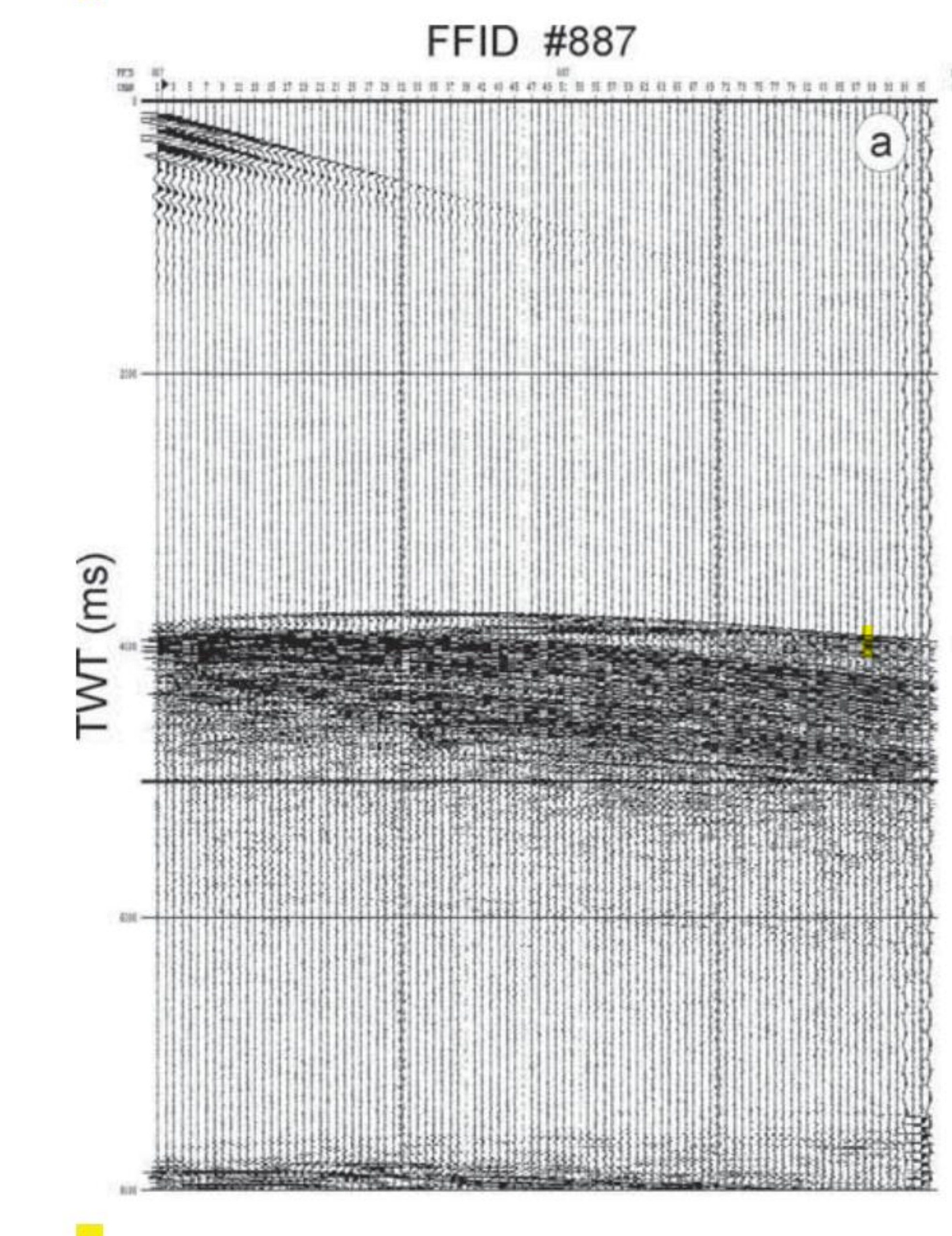
FFID #887
a
TWT (ms)

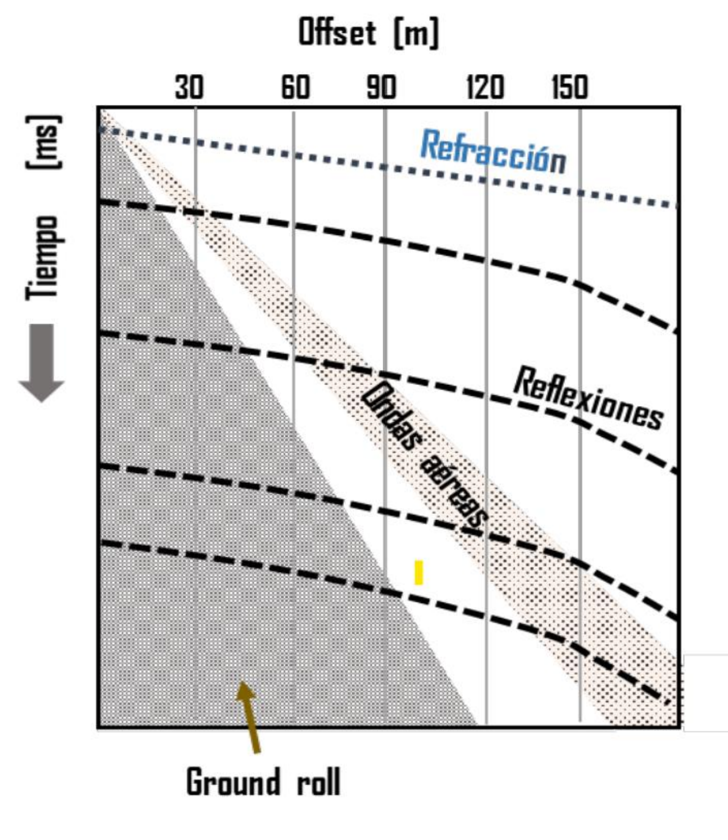

Offset [m]
30
60
90
120
150
Tiempo [ms]
Refracción
Reflexiones
Ondas aéreas
Ground roll

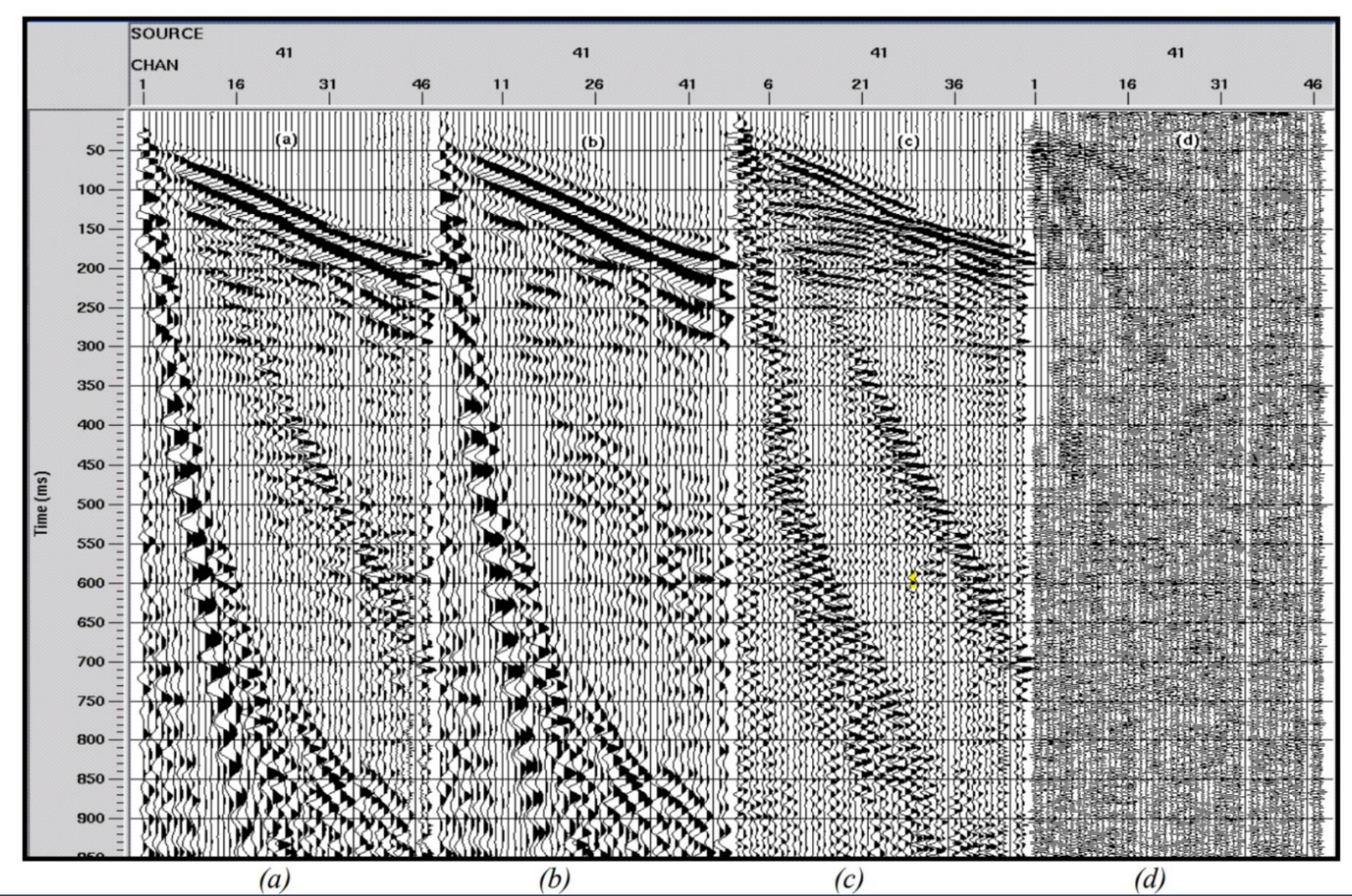

SOURCE
CHAN
41
1
16
31
46
11
26
41
6
21
36
Time (ms)
50
100
150
200
250
300
350
400
450
500
550
600
650
700
750
800
850
900
(a)
(b)
(c)
(d)

Sísmica de Refracción

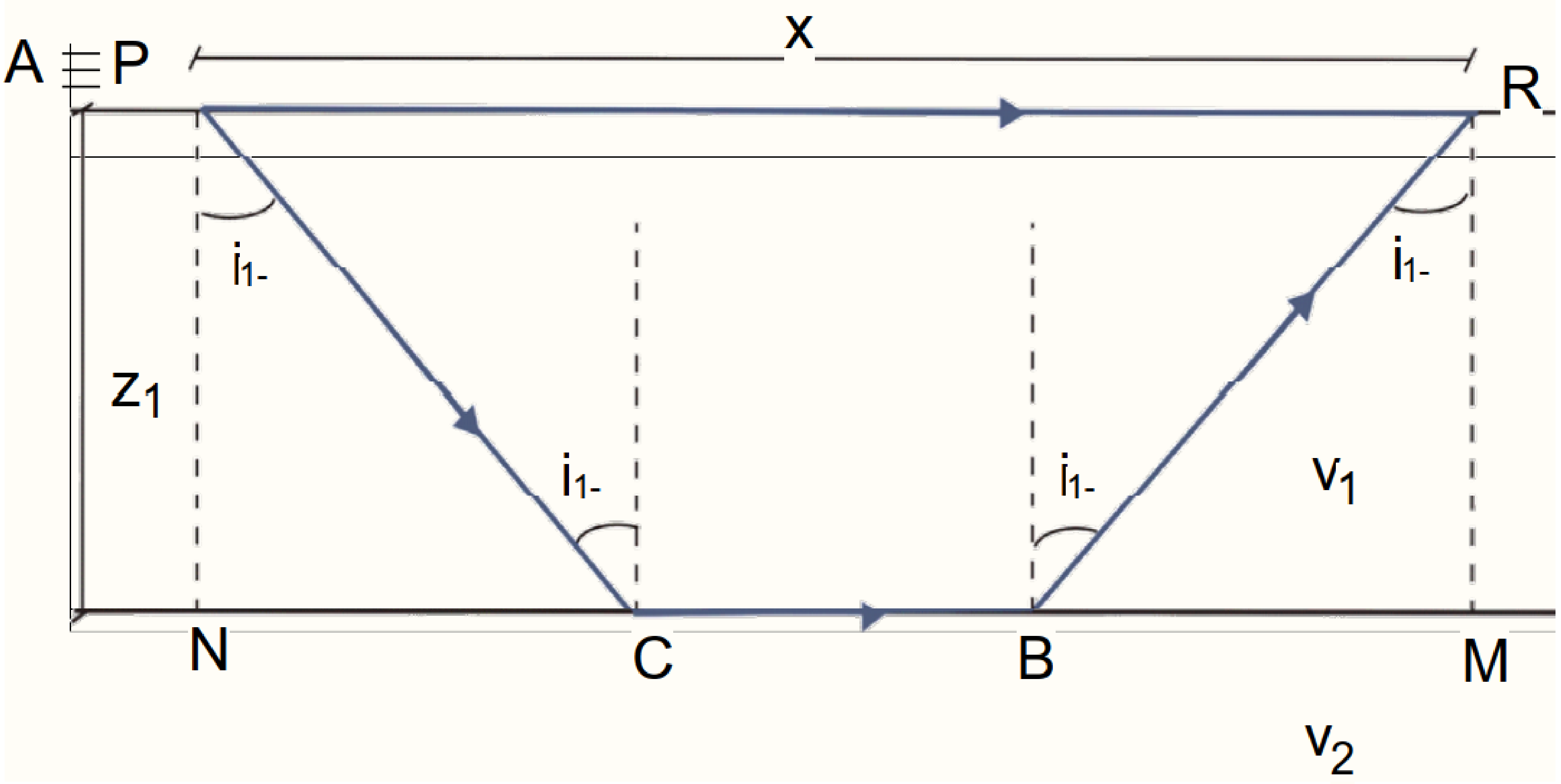

$$T_R = \frac{\overline{AC}}{v_1} + \frac{\overline{CB}}{v_2} + \frac{\overline{BR}}{v_1}$$

$$T_2 = \frac{x}{v_2} + \theta_2,$$ lo que representa una recta cuya pendiente es $1/v_2$ y la ordenada al origen θ_2

$t = m \cdot x + d$ (expresión matemática de una recta).

$$\theta_2 = \frac{2 \cdot z_1}{v_1} \cdot \cos(i_{1-2}),$$

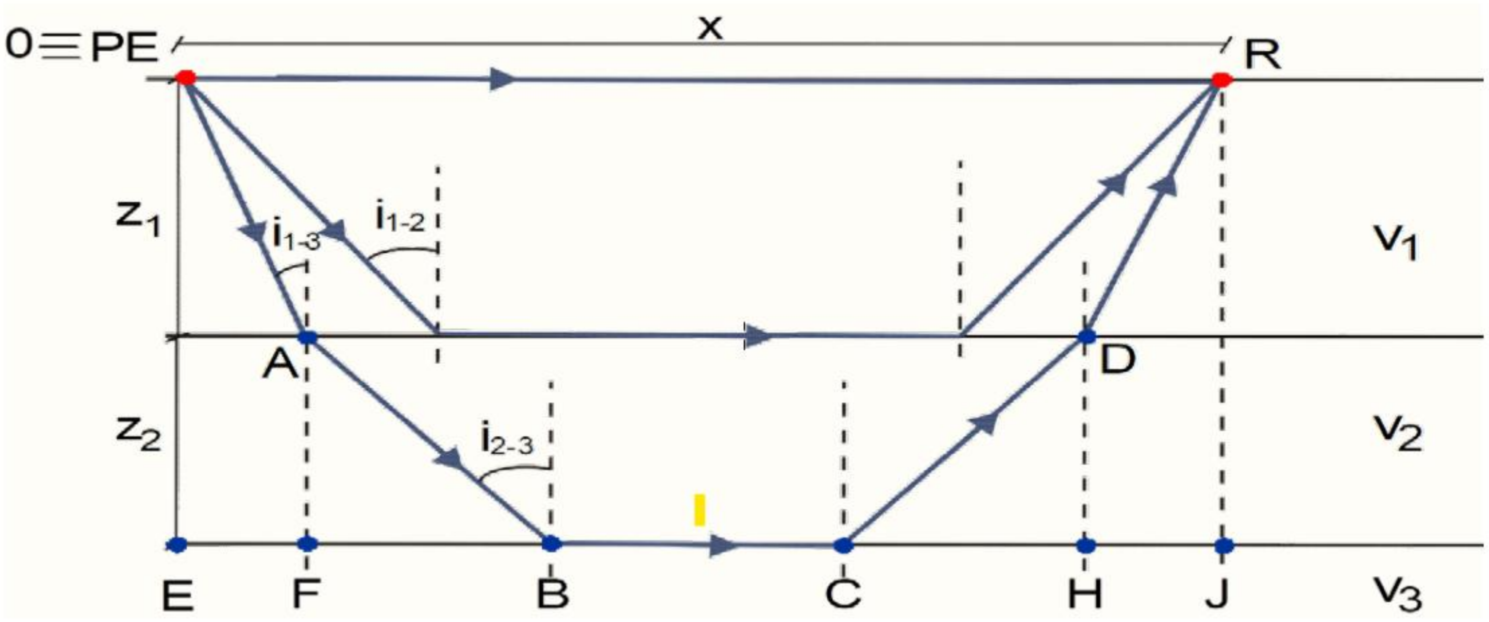

$$T_3 = \frac{x}{V_3} + \frac{2 \cdot z_1}{V_1} \cdot \cos(i_{1-3}) + \frac{2 \cdot z_2}{V_2} \cdot \cos(i_{2-3}),$$

θ_1 θ_2

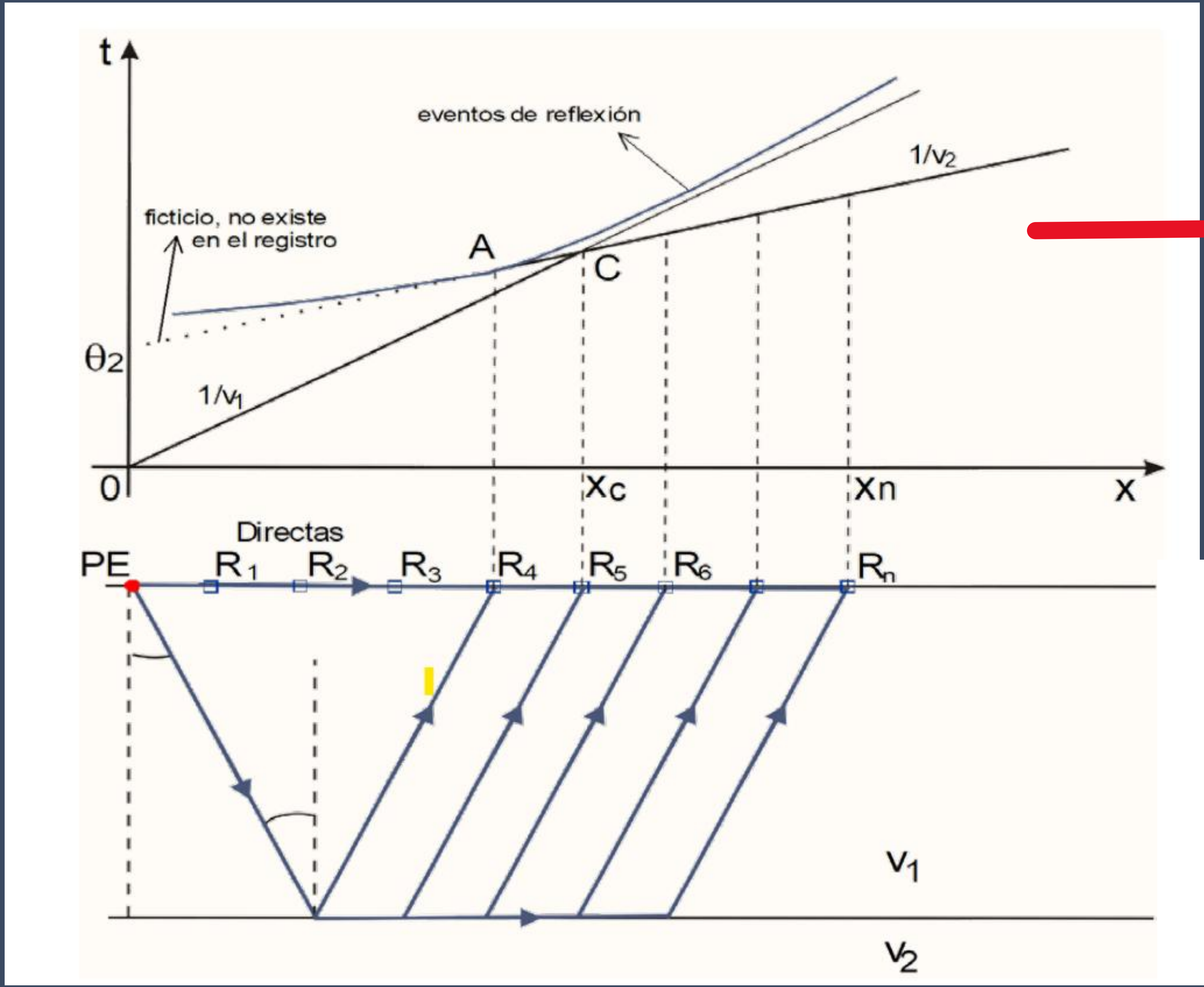

t
eventos de reflexión
$1/v_2$
ficticio, no existe
en el registro
A
C
θ_2
$1/v_1$
0
x_c
x_n
x
Directas
PE
R_1
R_2
R_3
R_4
R_5
R_6
R_n
v_1
v_2

Dromocrona

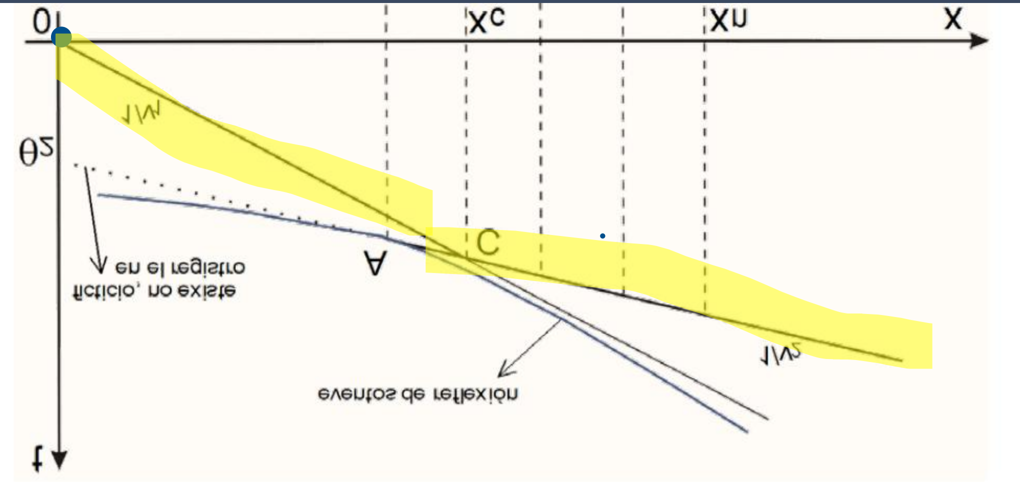

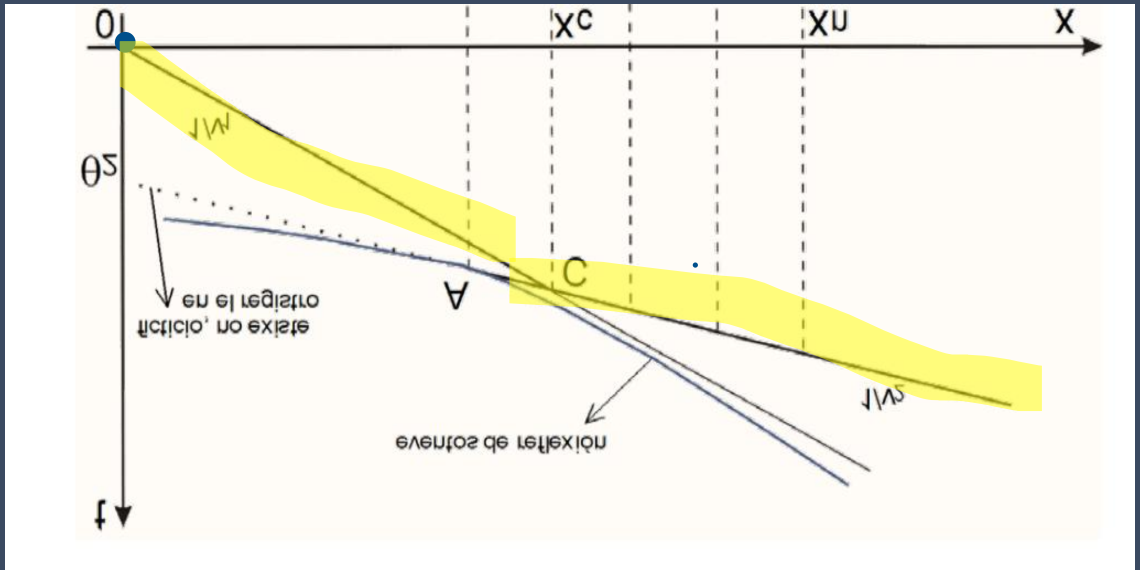

0
Xc
Xn
X
t
A
C
en el registro
ficticio, no existe
eventos de reflexion

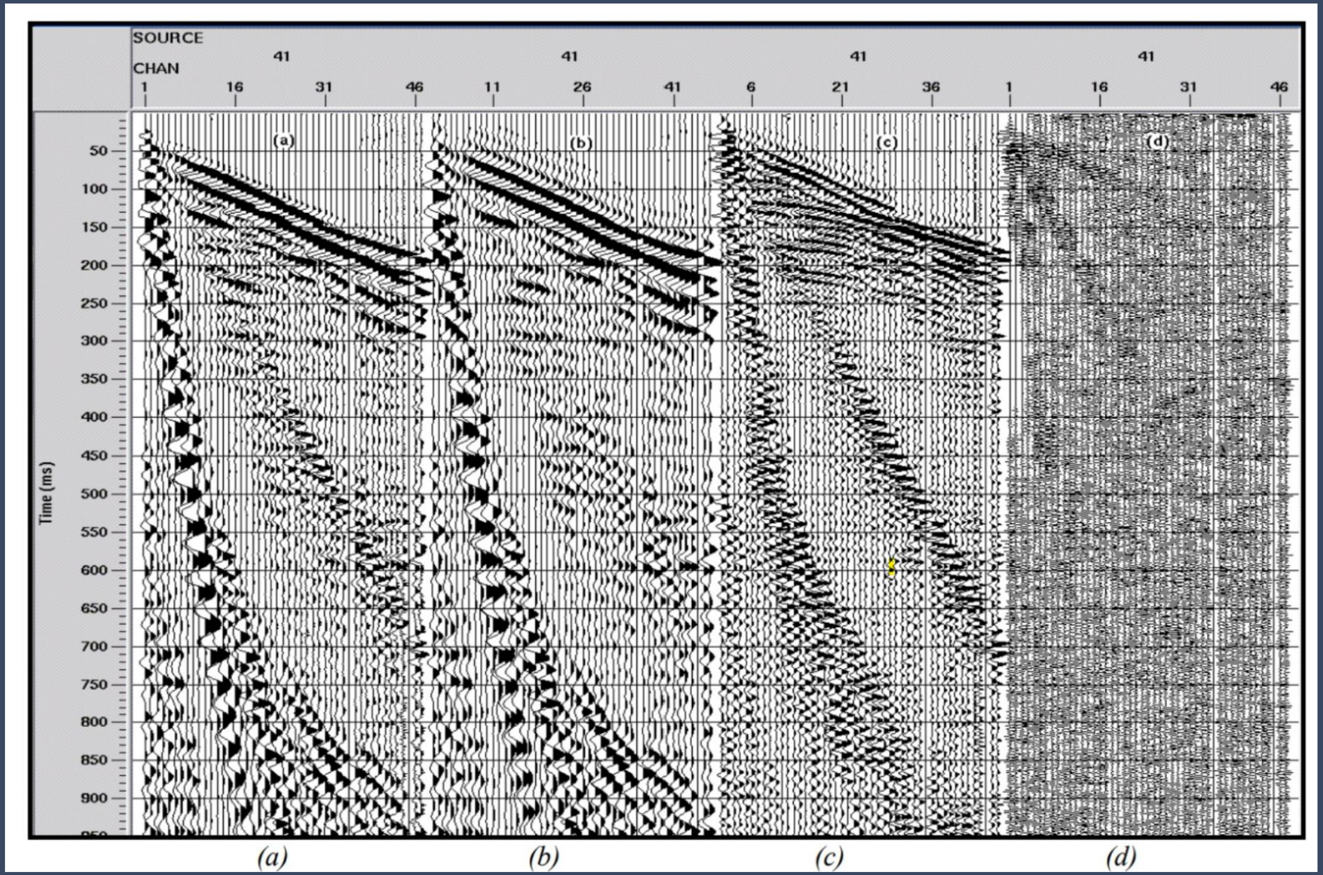

SOURCE
CHAN
41
1 16 31 46 11 26 41 6 21 36 1 16 31 46
Time (ms)
(a) (b) (c) (d)

¿Por qué dos?

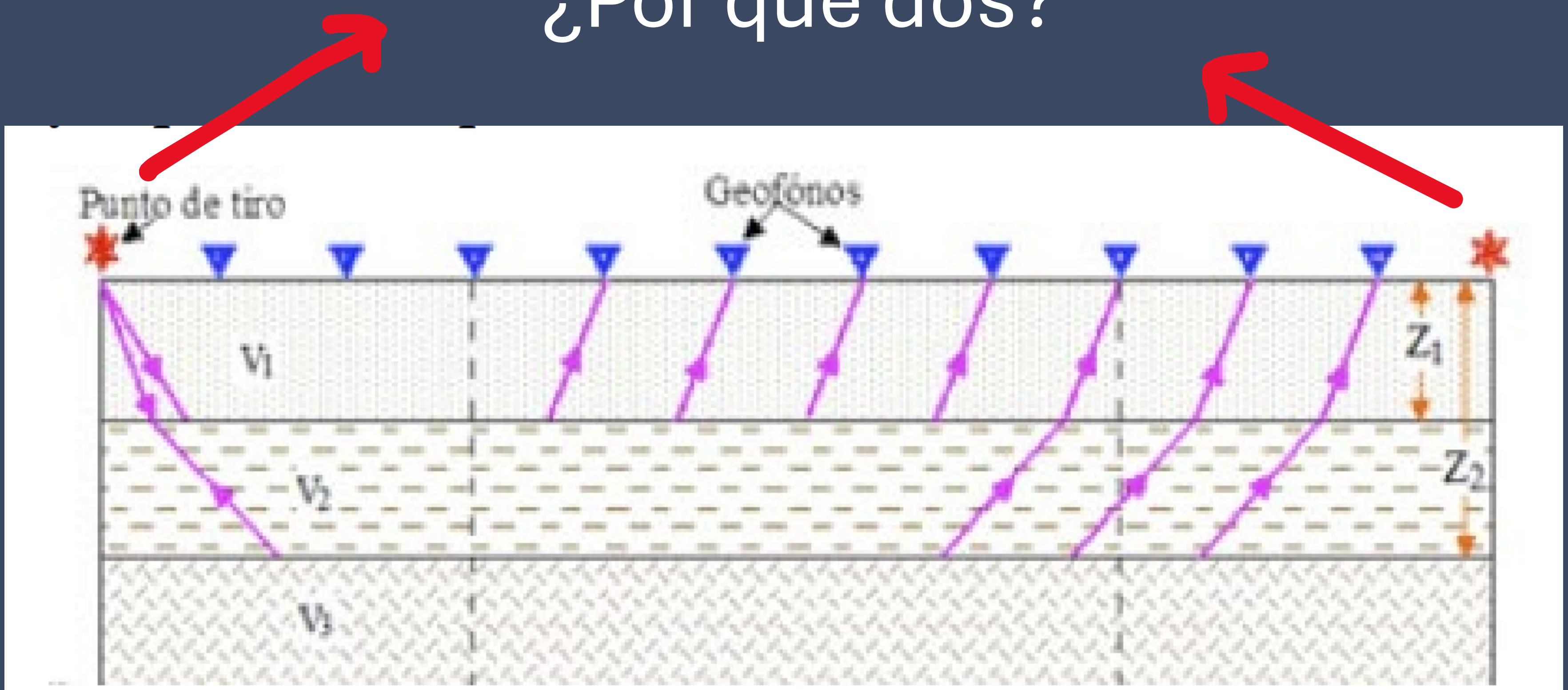

Figura N° 8: Arreglo de refracción asimétrico, con la ubicación del punto de tiro del perfil y del contraperfil. Distribución de receptores. Fuente de Imágenes: Modificado de Sheriff et al., 1991.

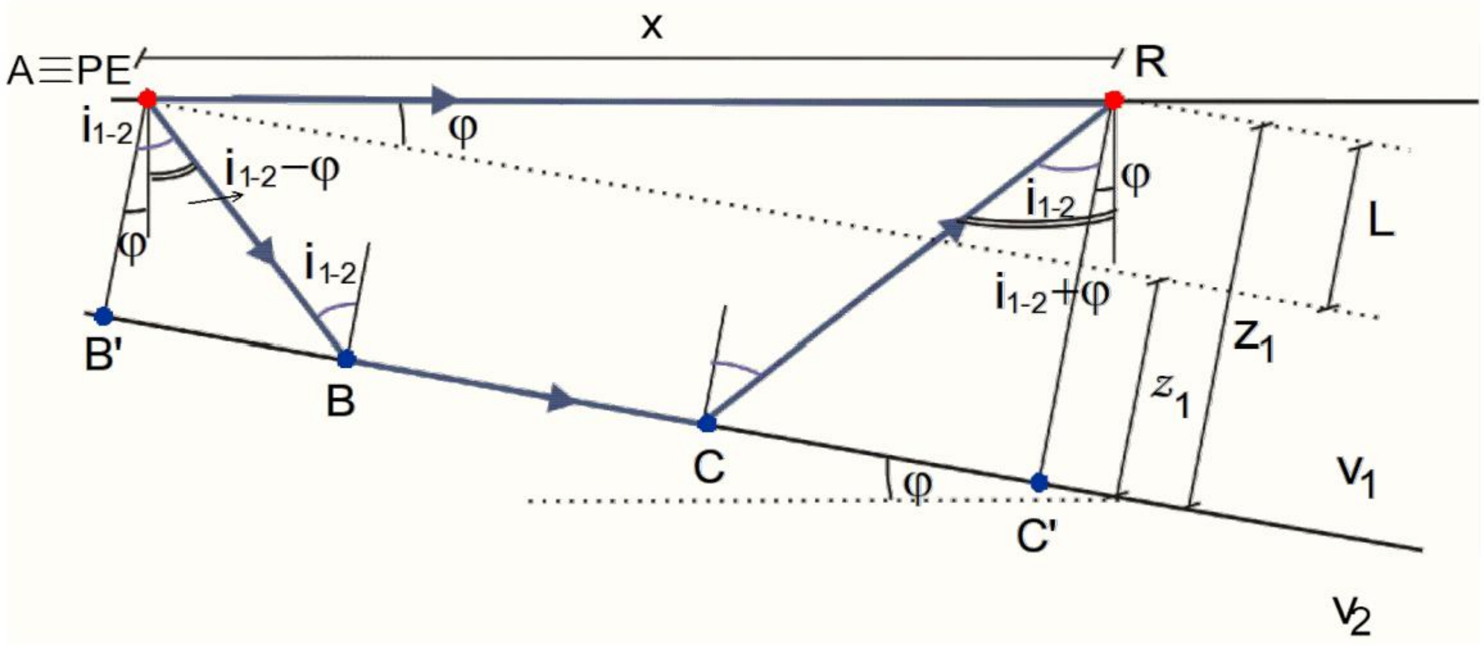

$T_{2b} = \frac{2 \cdot z_1}{v_1} \cdot \cos(i_{1-2}) + \frac{x}{v_1} \cdot \text{sen}(i_{1-2} + \varphi)$, llamando velocidad aparente de bajada a: $v_{2b} = \frac{v_1}{\text{sen}(i_{1-2} + \varphi)}$

este término es θ_{2b}

$T_{2s} = \frac{2 \cdot z_1}{v_1} \cdot \cos(i_{1-2}) + \frac{x}{v_1} \cdot \text{sen}(i_{1-2} - \varphi)$, llamando velocidad aparente de subida a: $v_{2s} = \frac{v_1}{\text{sen}(i_{1-2} - \varphi)}$

este término es θ_{2s}

$$v_{2b} = \frac{v_1}{\text{sen}(i_{1-2} + \varphi)} < v_{2Real} = \frac{v_1}{\text{sen}(i_{1-2})} < v_{2s} = \frac{v_1}{\text{sen}(i_{1-2} - \varphi)}$$

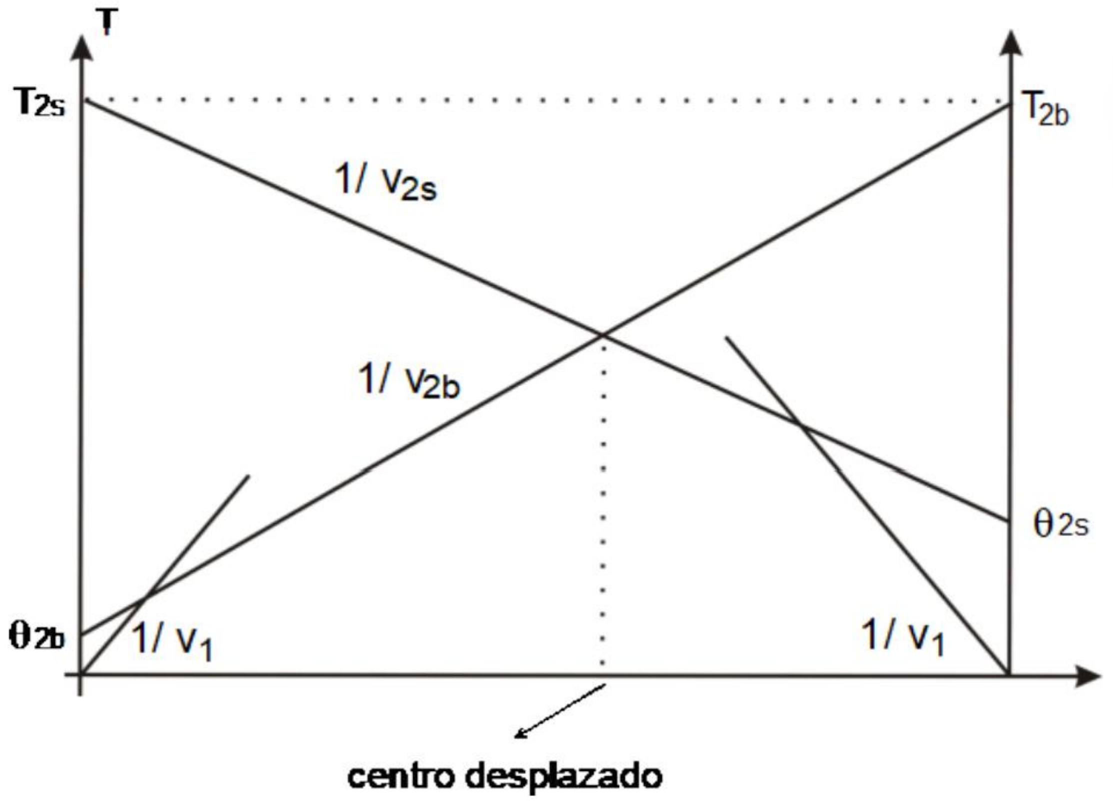

Figura N°13: Dromocrona del Perfil y contraperfil para un sistema de 1 capa inclinada.

$$v_{2b} = \frac{v_1}{sen(i_{1-2} + \varphi)} < v_{2Real} = \frac{v_1}{sen(i_{1-2})} < v_{2s} = \frac{v_1}{sen(i_{1-2} - \varphi)}$$

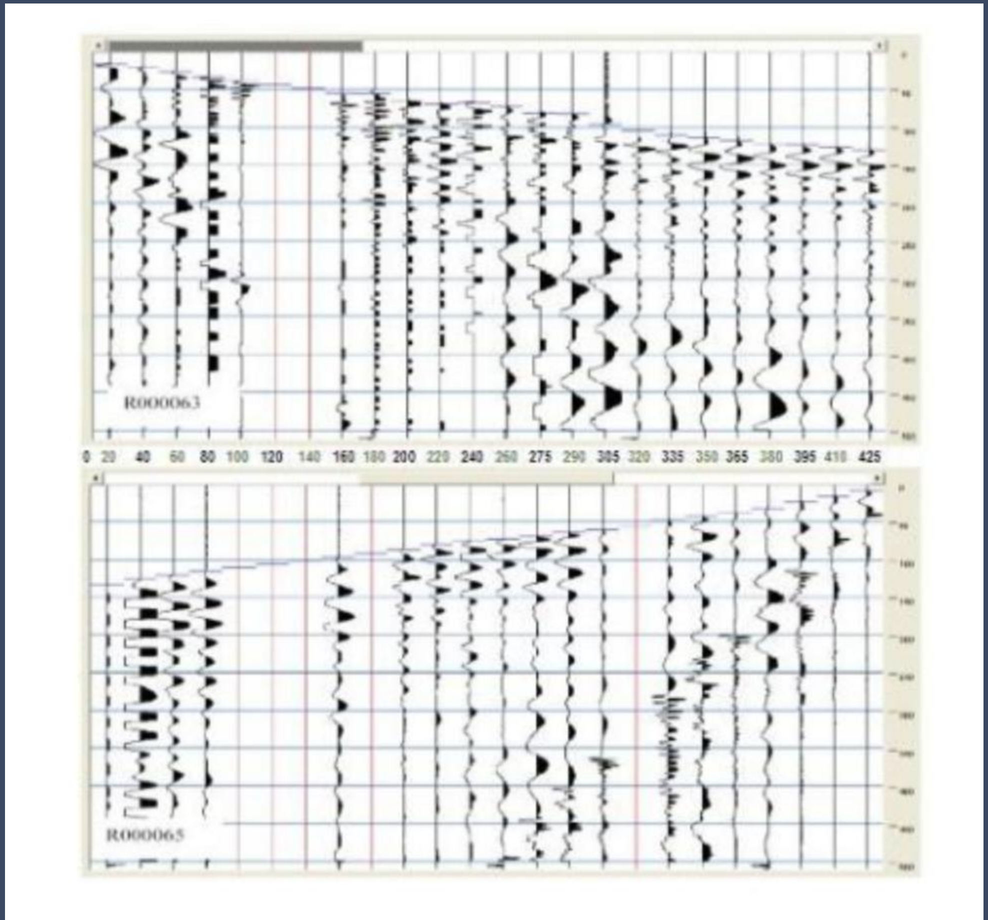

	Tiempo	
Distancia	Perfil	Contra Perfil
0	0	
20	12	130
40	20	125
60	25	123
80	30	120
100	37	
120		
140		
160	57	98
180	60	90
200	68	80
220	70	78
240	73	75
260	75	72
275	78	70
290	80	66
305	90	63
320	105	
335	110	50

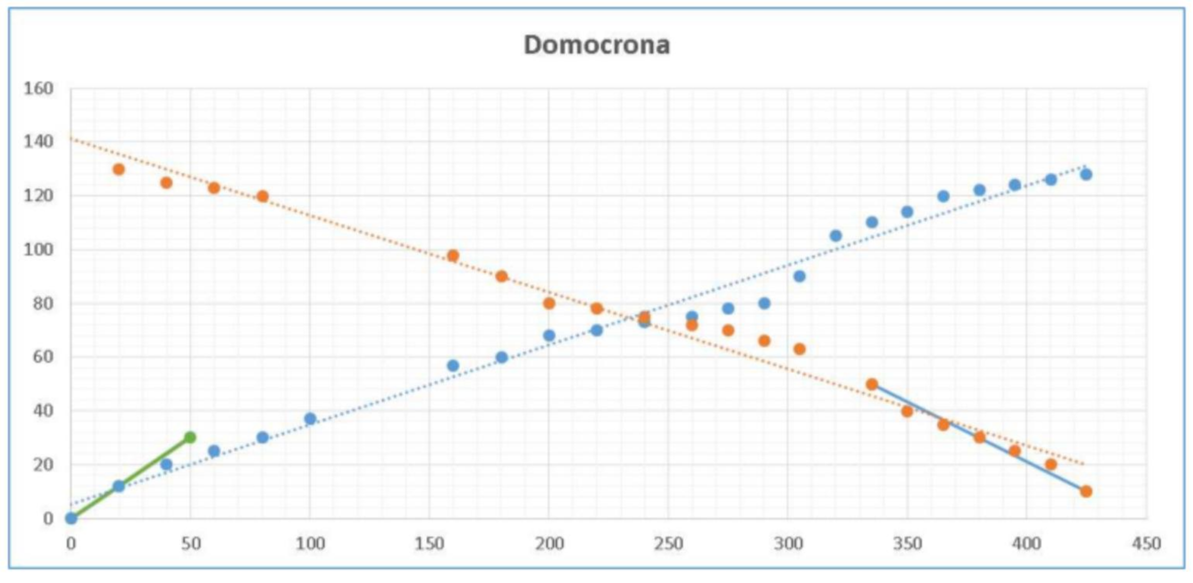

Sísmica de Reflexión

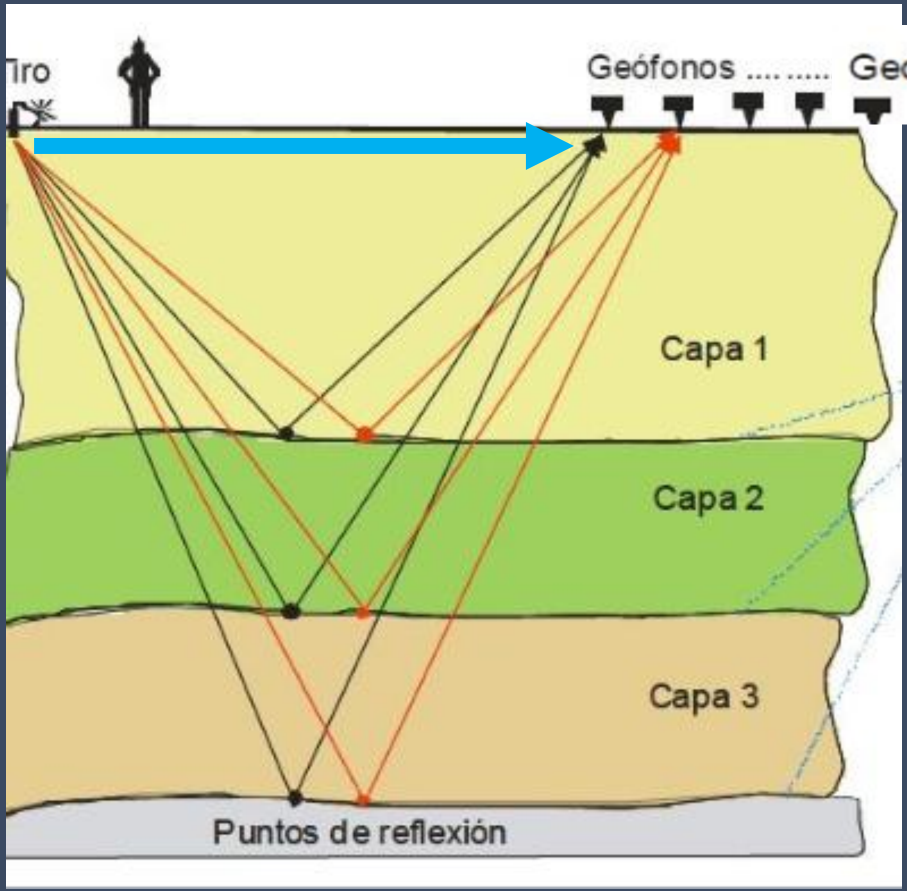
Tiro
Geófonos .... Geófonos ....
Capa 1
Capa 2
Capa 3
Puntos de reflexión
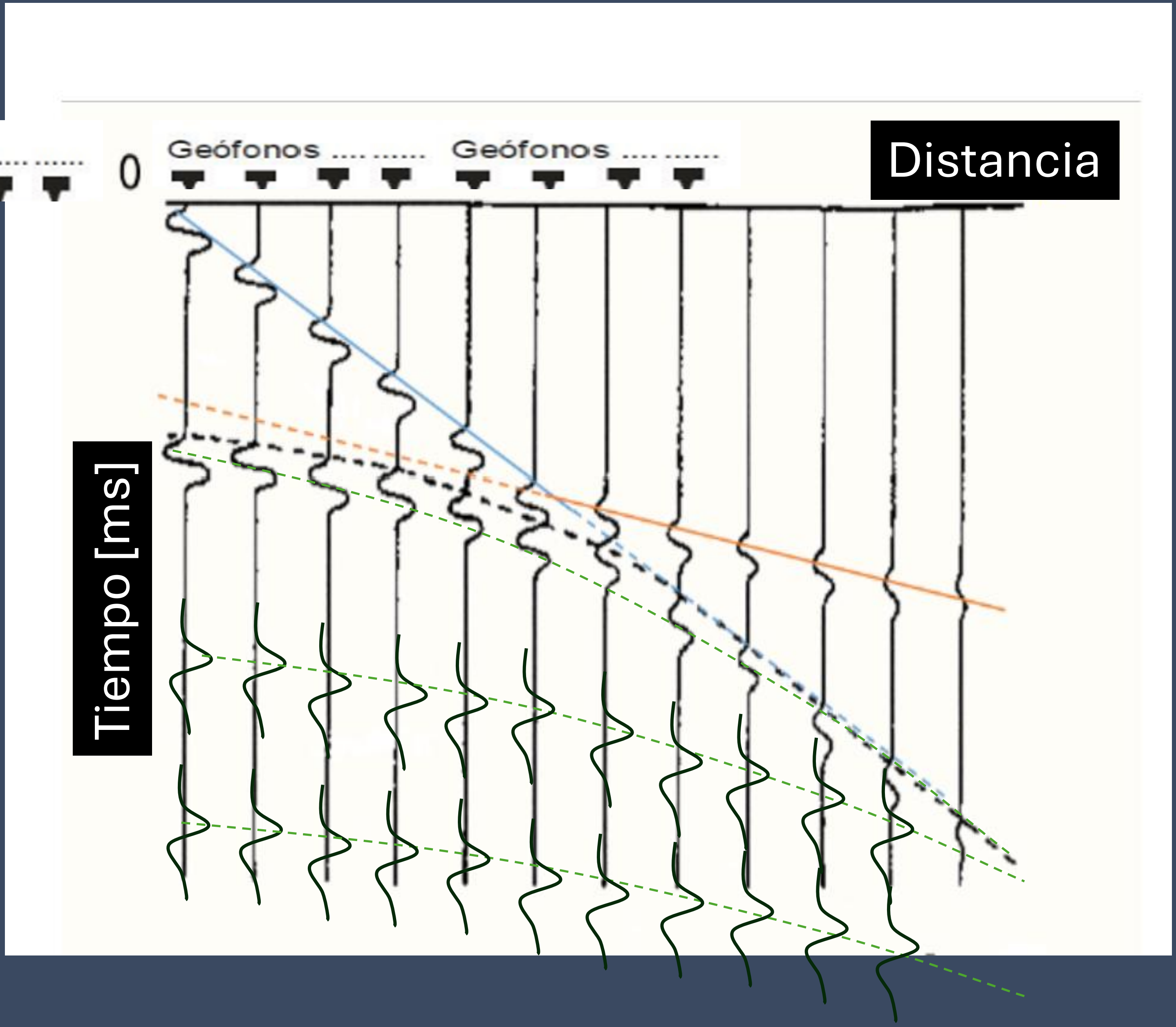
0
Geófonos .... Geófonos ....
Distancia
Tiempo [ms]

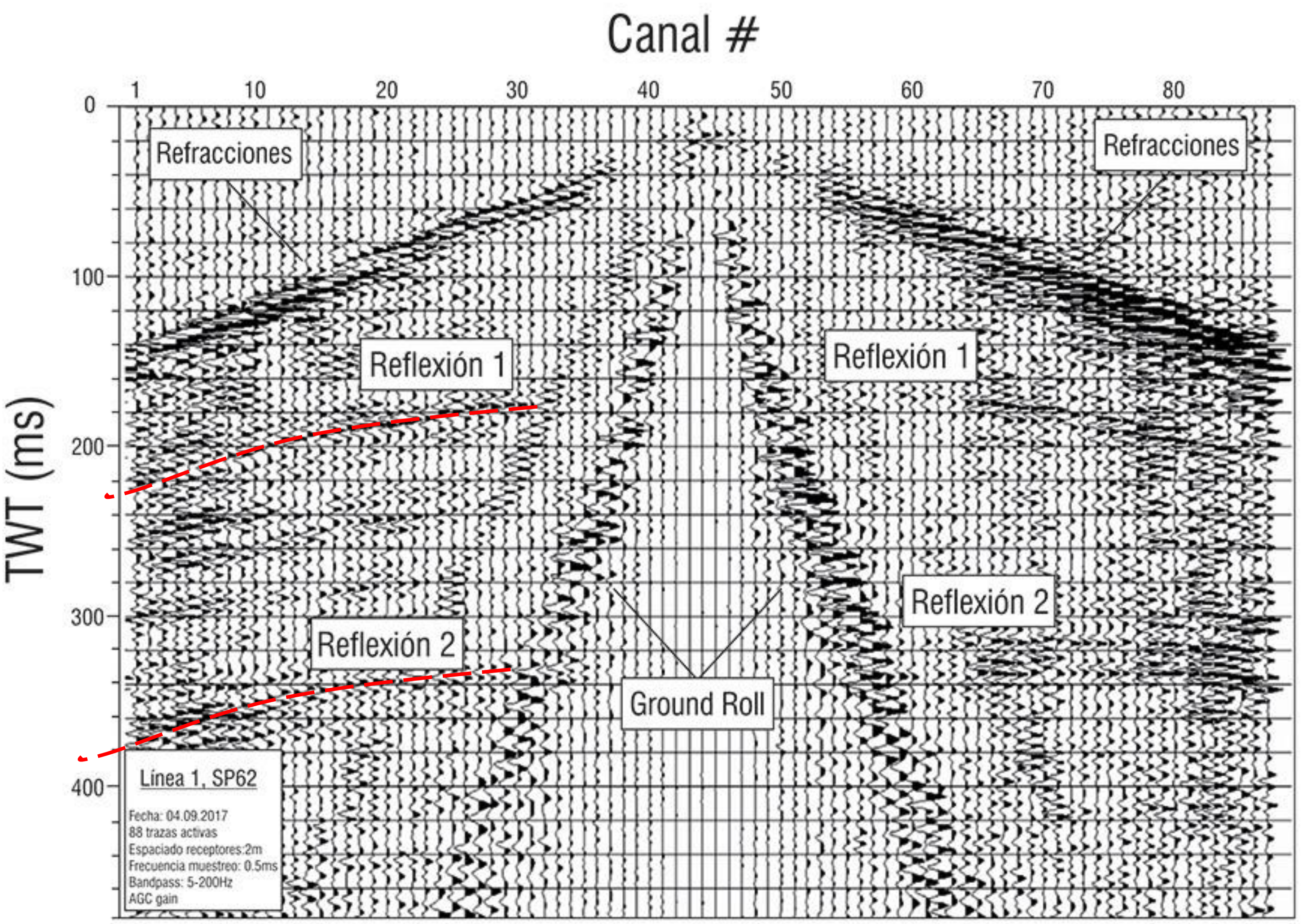
Canal #
1
10
20
30
40
50
60
70
80
TWT (ms)
0
100
200
300
400
Refracciones
Refracciones
Reflexión 1
Reflexión 1
Reflexión 2
Reflexión 2
Ground Roll
Línea 1, SP62
Fecha: 04.09.2017
88 trazas activas
Espaciado receptores:2m
Frecuencia muestreo: 0.5ms
Bandpass: 5-200Hz
AGC gain

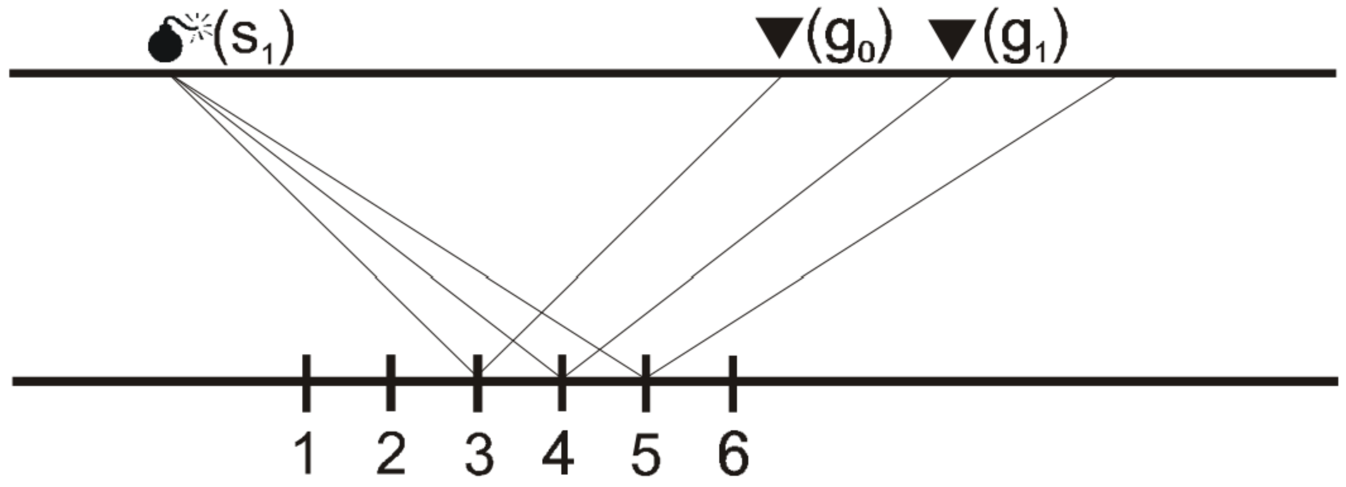

Figura b

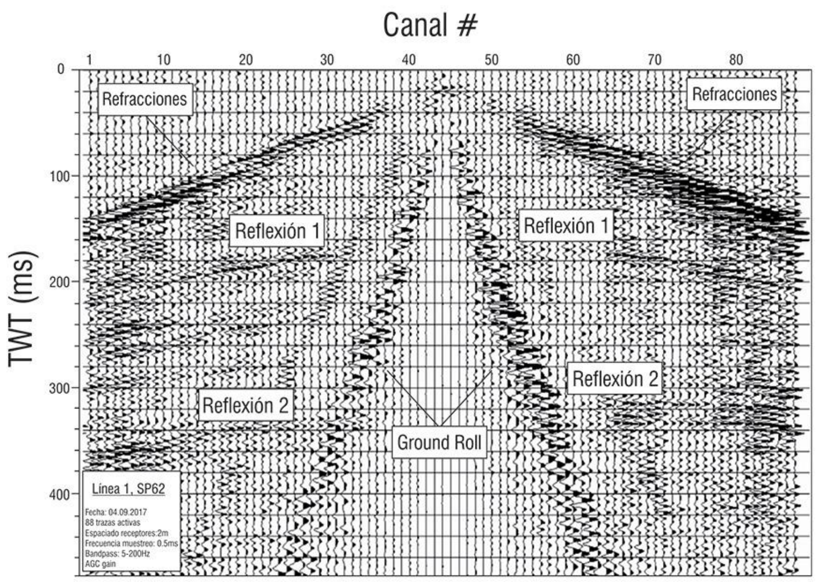

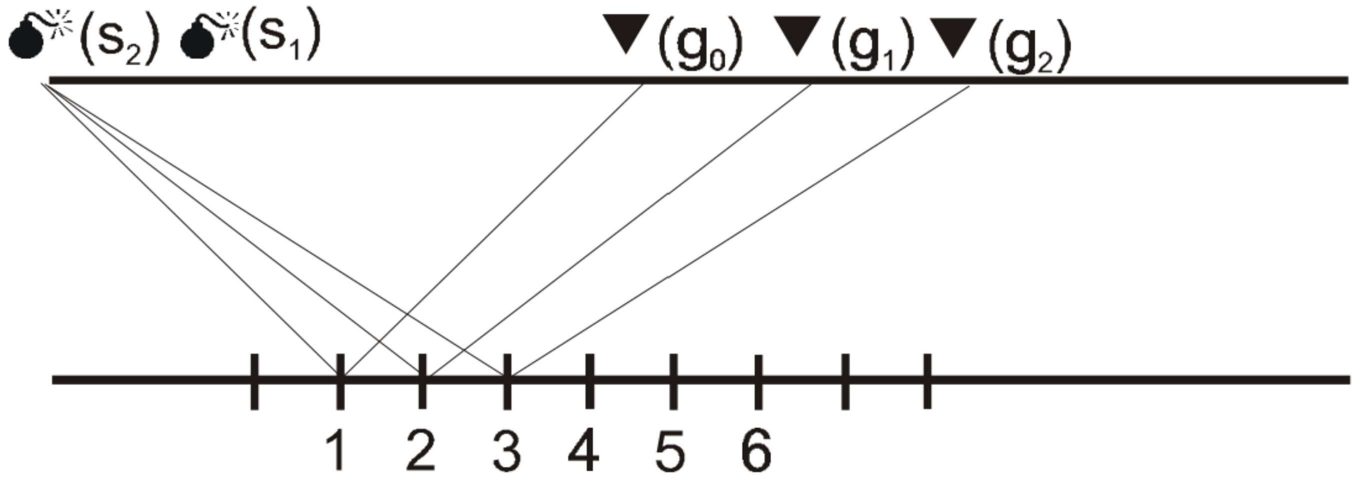

Figura c

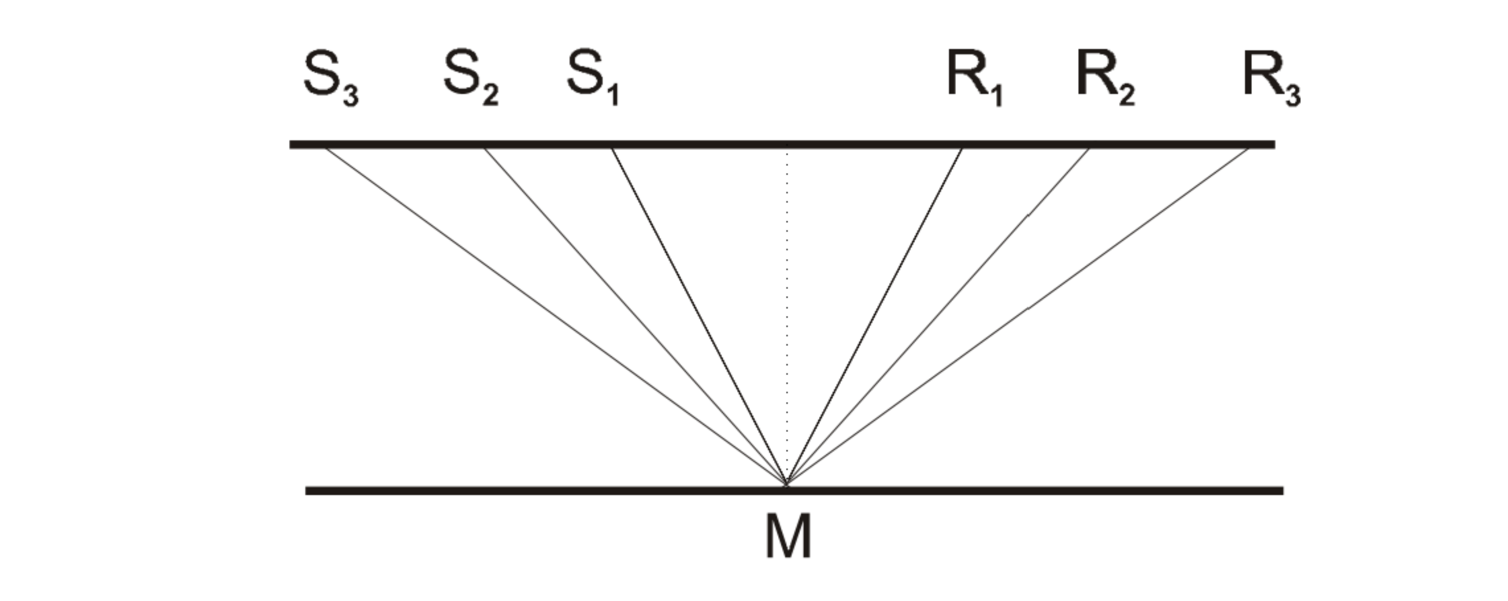

$$t^2(x) = t^2(0) + \frac{x^2}{v^2}$$

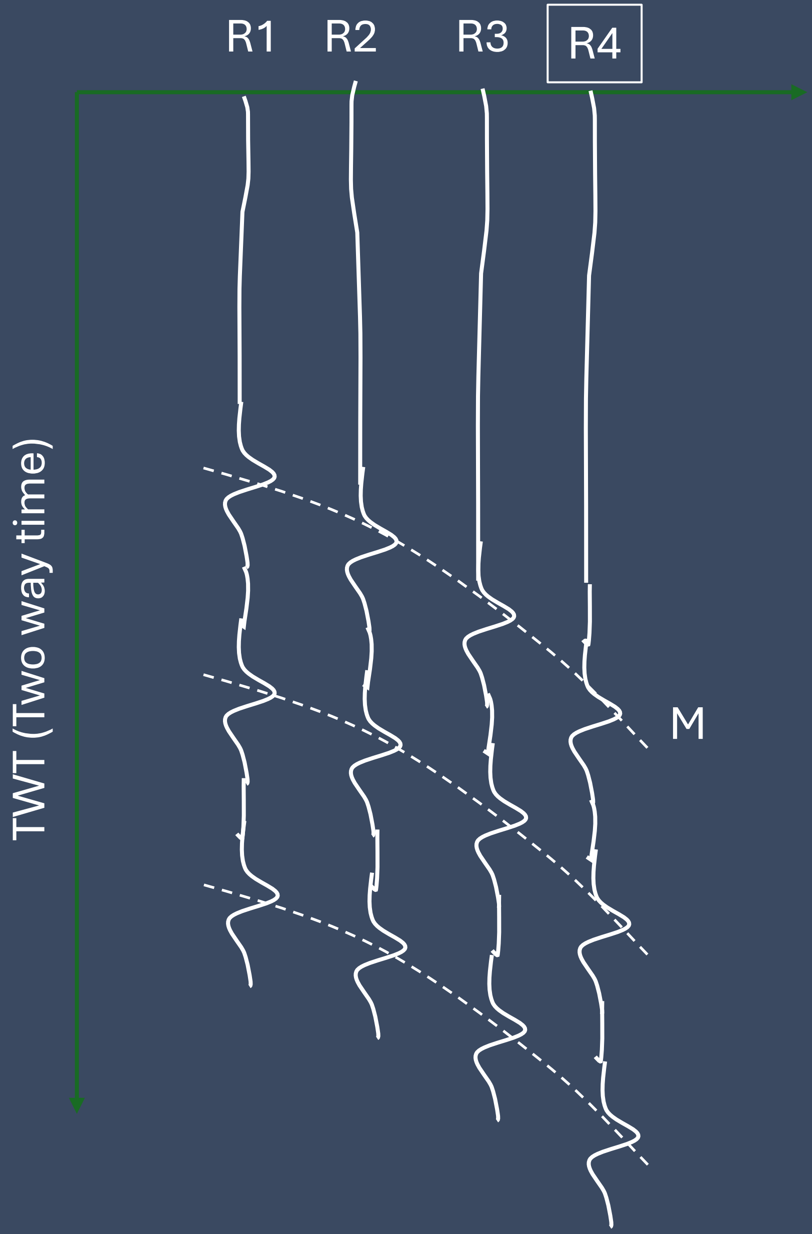

Correcciones NMO (Normal Move Out) y Stacking

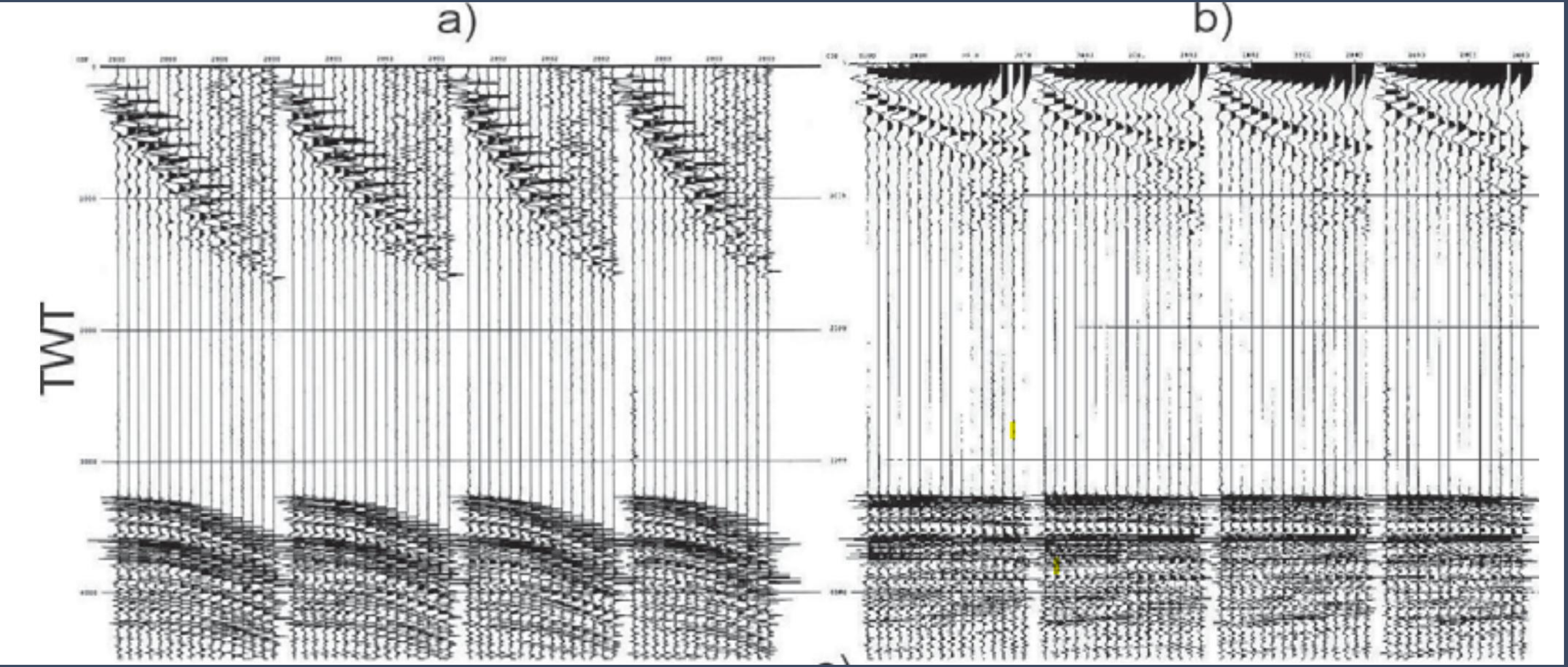

Convolución - Deconvolución

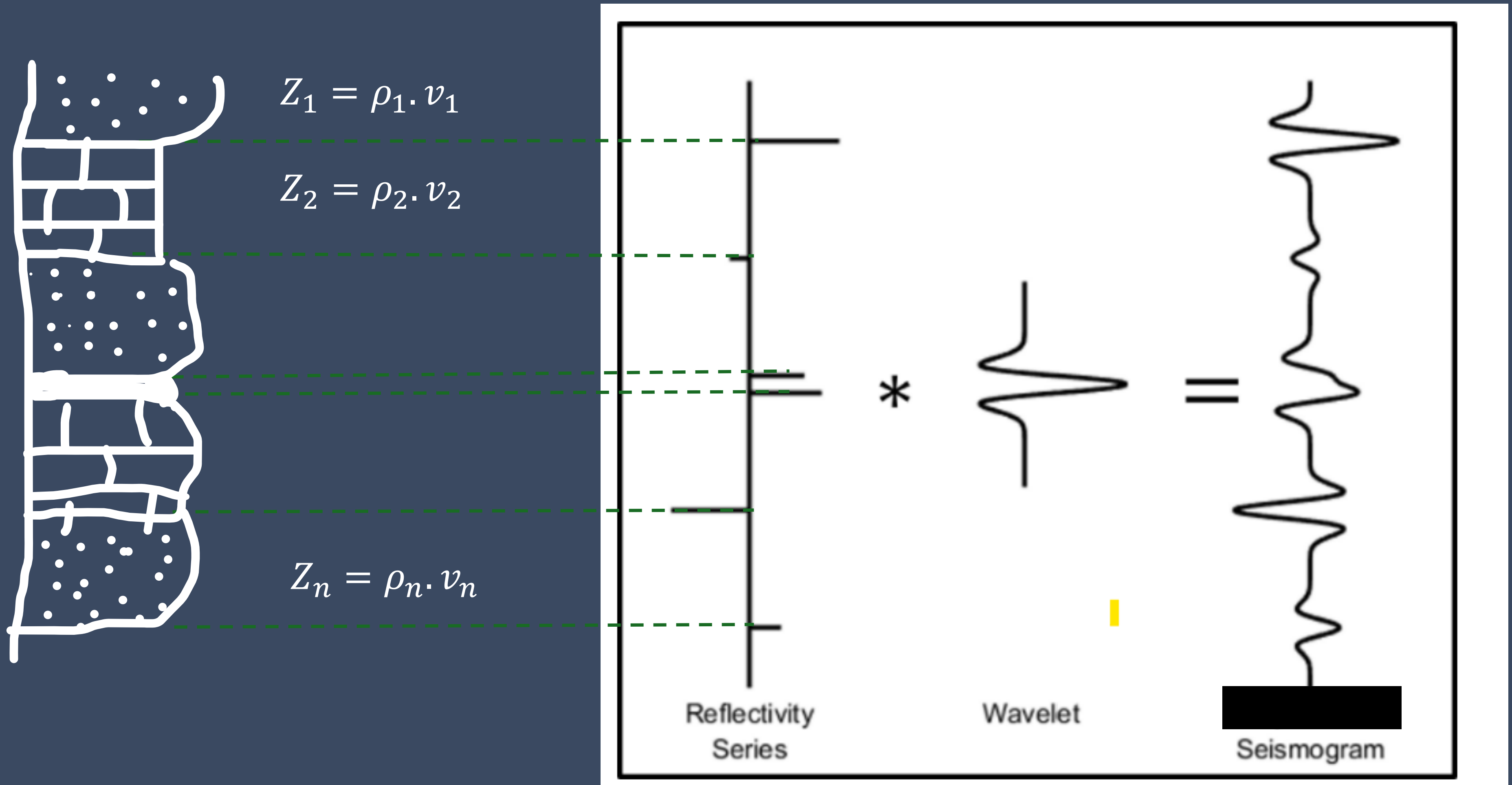

Figure 1. Synthetic seismogram modeling based on Eq. 1.

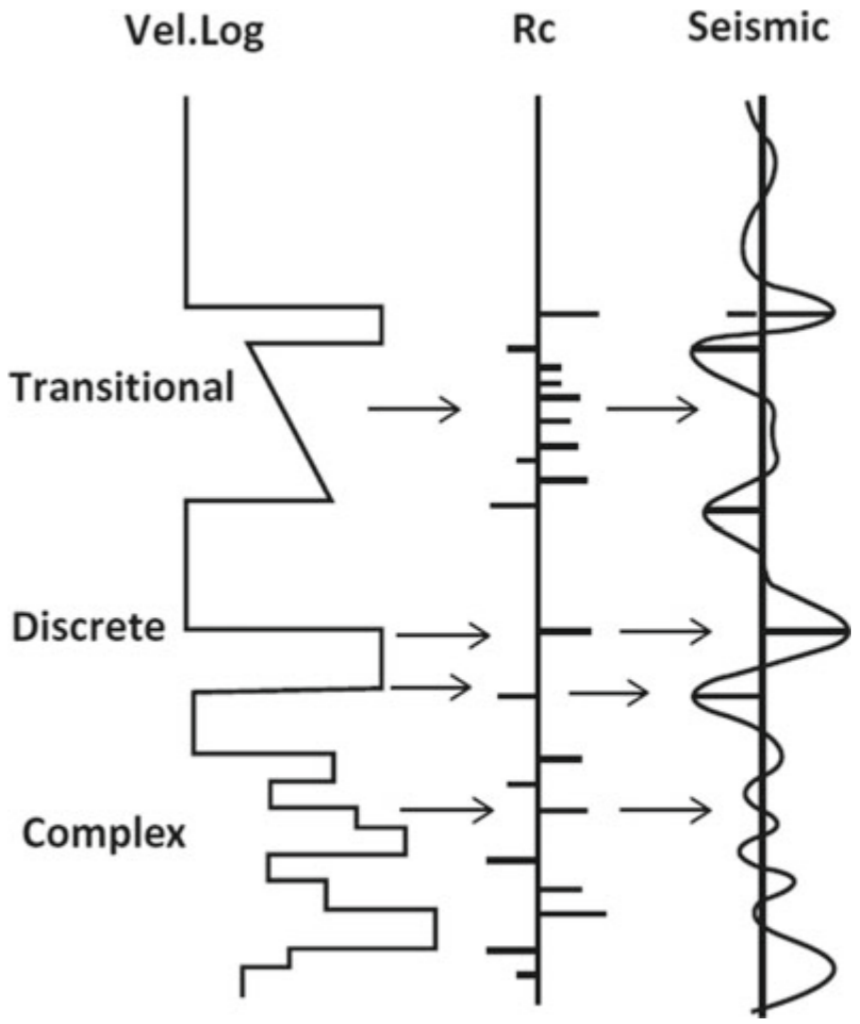

Fig. 10 Schematic showing the different types of reflectors. A 'discrete' reflector causes top and bottom reflections, resolvable with distinctive polarity and exact arrival time. The 'transitional' and 'complex' reflectors are composite events of several closely spaced beds with uncertain signage of polarity and delayed arrival time

Resolución Vertical

Resolución: capacidad de separar dos rasgos distintos en tiempo (profundidad) y distancia lateral (Nanda, 2021).

Figure 2.29: Schematic representation of the convolutional theorem

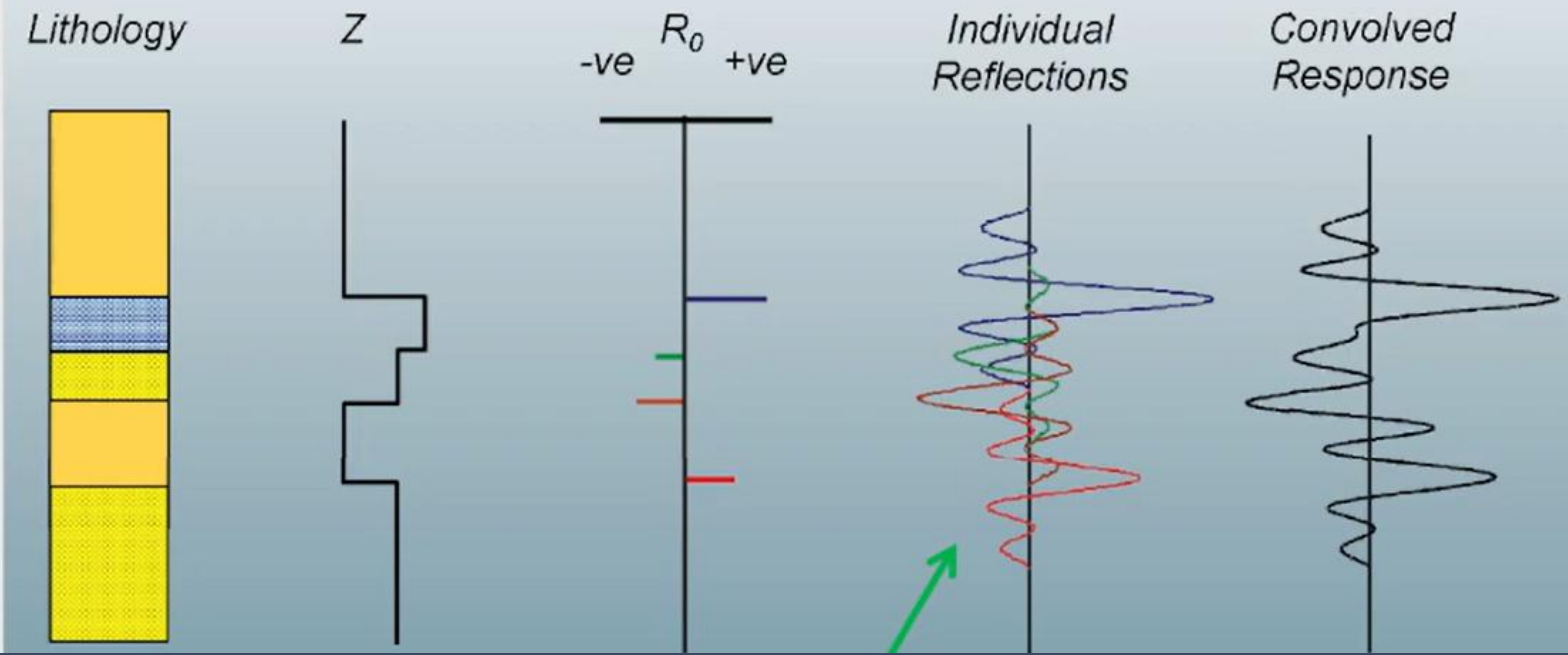

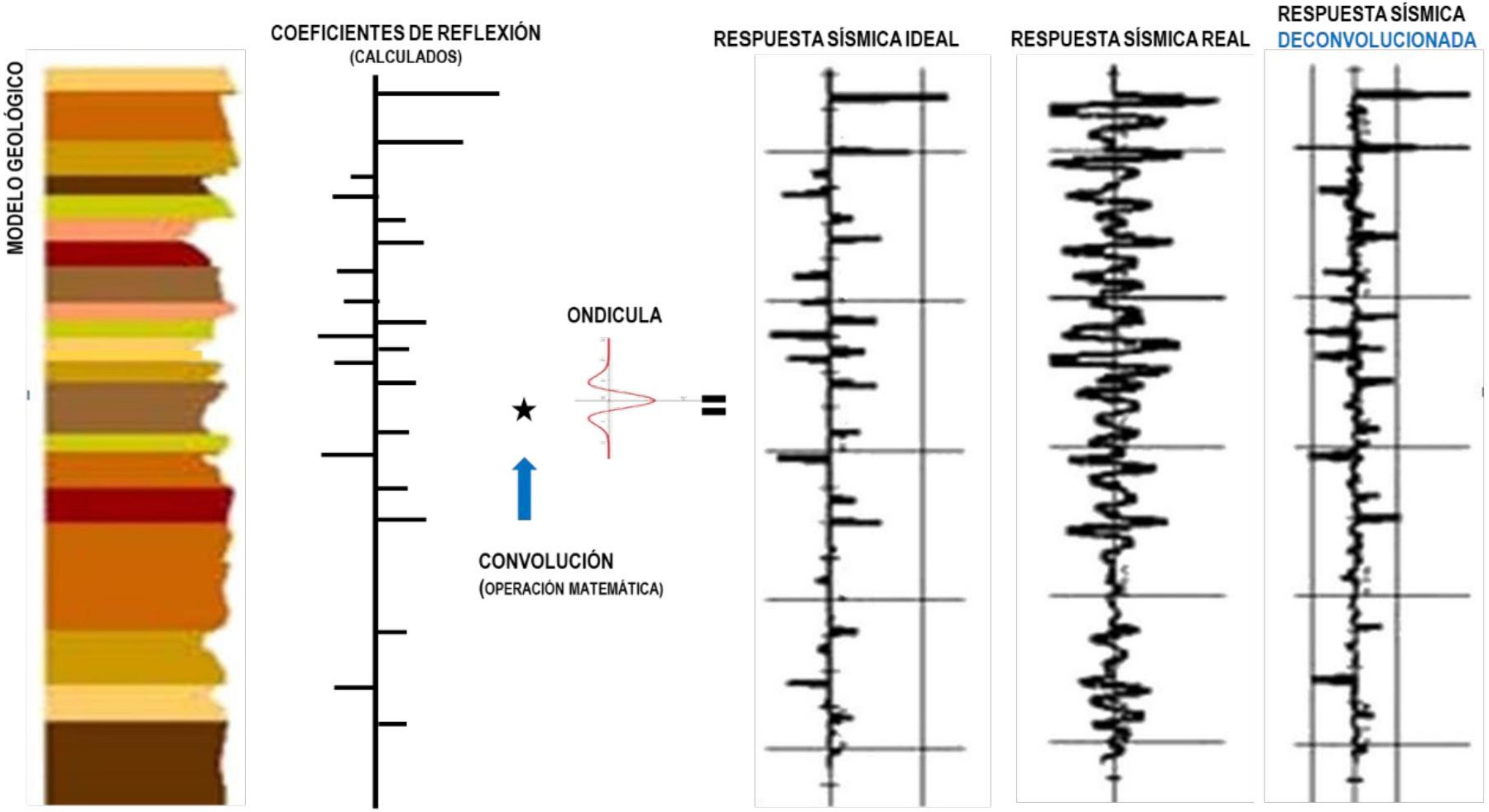

Figura N° 18: esquema del proceso de convolución de la ondicula con el modelo geológico, dando

Resolución vertical

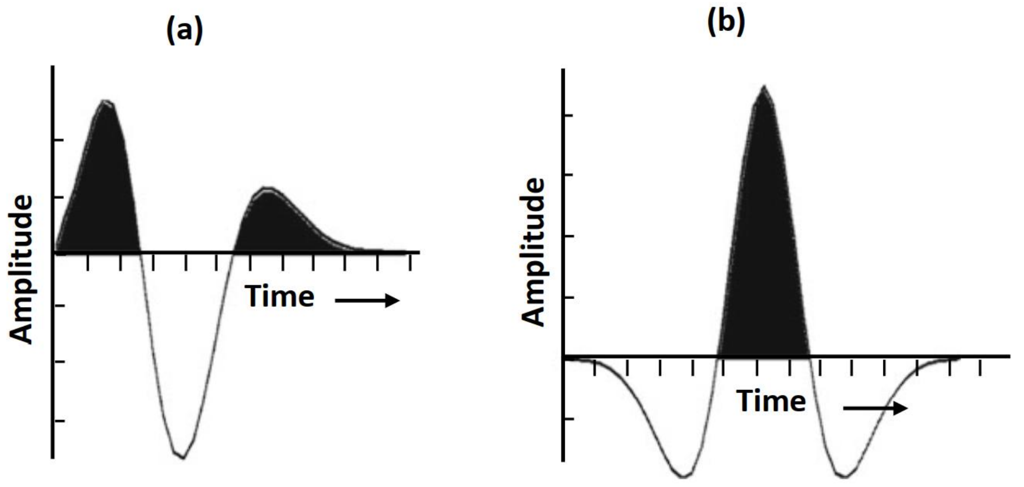

Fig. 2 Showing types of seismic source wavelet types (**a**) minimum phase wavelet, generated by dynamite on land and air-gun in offshore and (**b**) zero phase wavelet generated by Vibroseis in land data acquisition. Zero phase wavelet is symmetrical with even side lobes and the amplitude maxima occurs at time corresponding to exact depth of the strata without time delay. Note the minimum phase wavelet (**a**) is asymmetrical with energy loaded in front and the maxima occurs at a delayed time

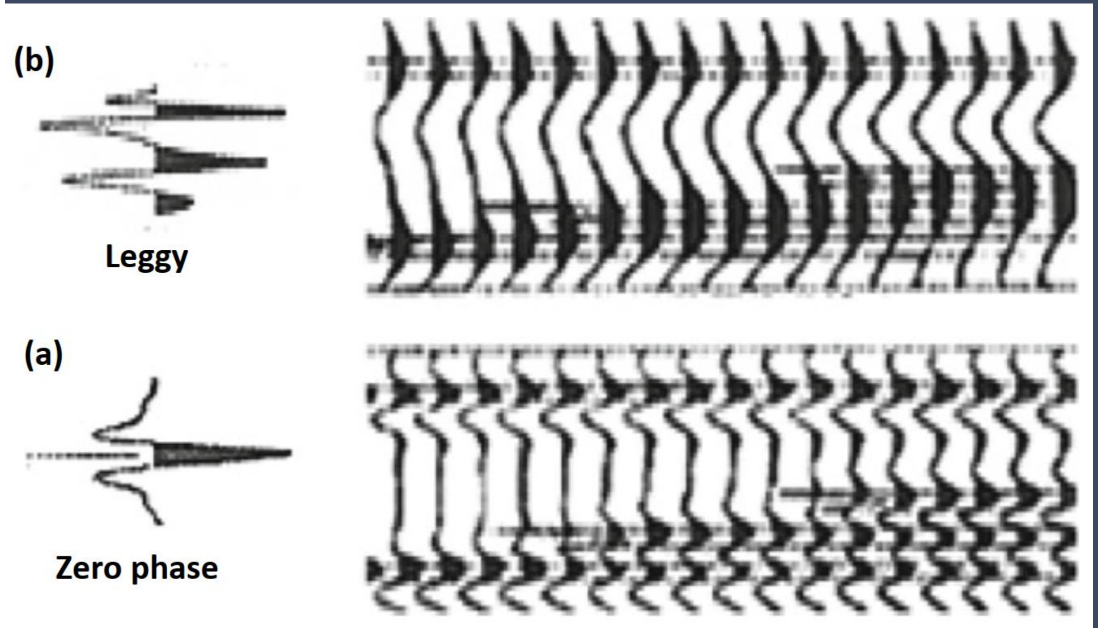

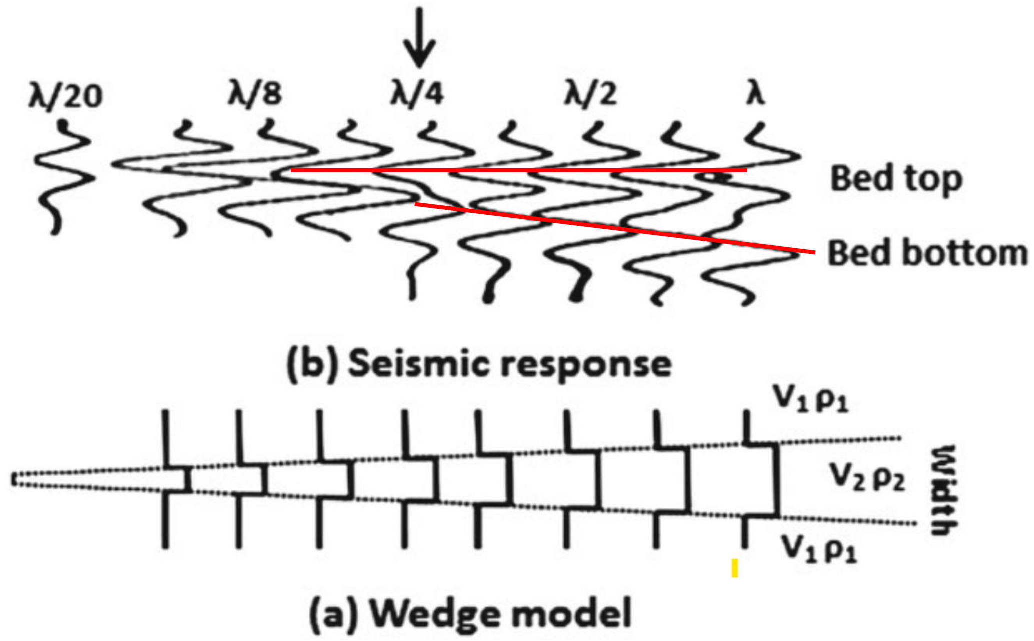

Fig. 4 Schematic illustrating Widess wedge model for vertical resolution limits. (**a**) The Widess wedge model and (**b**) seismic response for varying bed thickness. For a bed thickness greater or equal to the wave length (λ), the top and bottom reflections are clearly resolvable and are so till quarter wave length (λ/4). For beds thinner than λ/4 the top and bottom reflections are not distinct (arrow marked), limiting the vertical resolution to quarter wave length (after Widess 1973)

$$\lambda = \frac{v}{f}$$

velocidad

Frecuencia
10Hz – 70Hz

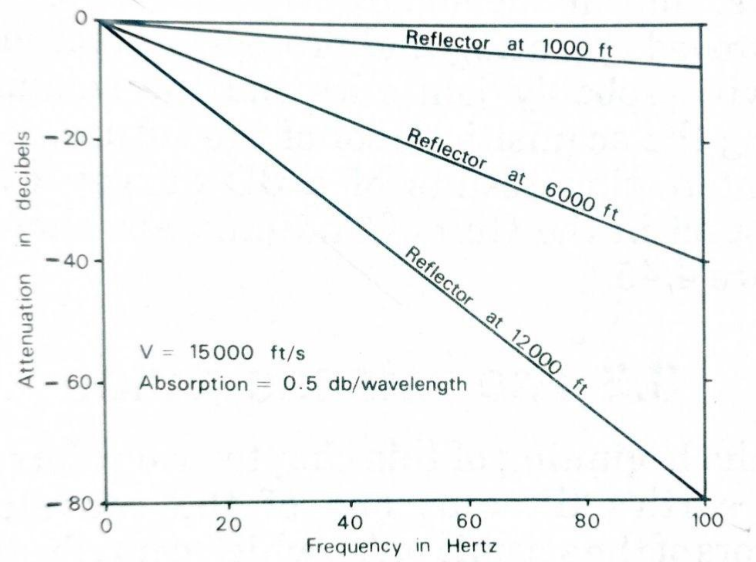

Figure 3/12 The effect of absorption in reducing seismic bandwidth with depth of a reflector. High frequencies are severely attenuated in the spectrum of deep reflections (after Evenden *et al*., 1971).

λ = 2000 m/s ÷ 40 Hz = 50 metros

Velocidad promedio en sedimentos

Figure 2.31: Schematic representation of a wedge model

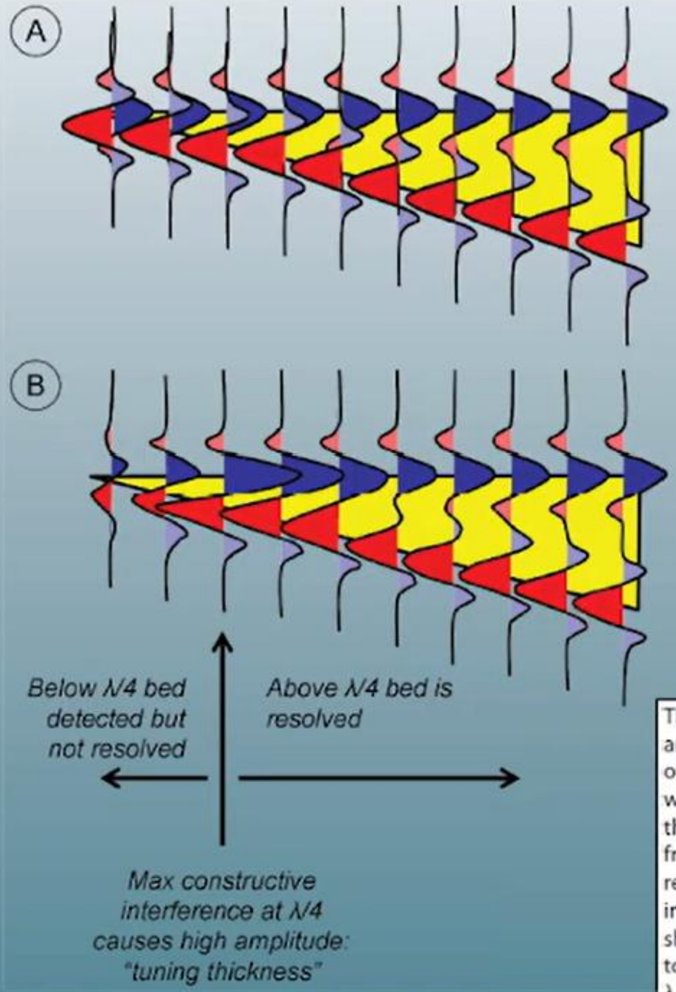

Top and base of wedge generate reflections. Amplitude of those reflections does not change along wedge.

Convolutional response. Constructive and destructive interference cause changes in amplitude and reflection shape.

The upper image shows the individual reflections that would be genera
and base of the wedge based on their respective reflection coefficients.
of the reflections does not change laterally because the acoustic imped
wedge, and the layers above and below the wedge, does not change. N
that in the middle and on the right there will be interference between t
from the top and base of the wedge. The lower image shows the convo
response (i.e. what would be recorded seismically). Constructive and de
interference between the reflections at the top and base causes change
shape and amplitude. When the bed thickness is $\lambda/4$, constructive inter
top and base of the bed cause an amplitude maximum, known as a tuni
$\lambda/4$ the amplitude of the reflections decreases because of destructive in
below $\lambda/4$ it is no longer possible to separate the reflection from the top
the reflection from the base. The bed is detected, although not resolve

Image from Hart textbook


LOOKOFFICE

Resolución horizontal

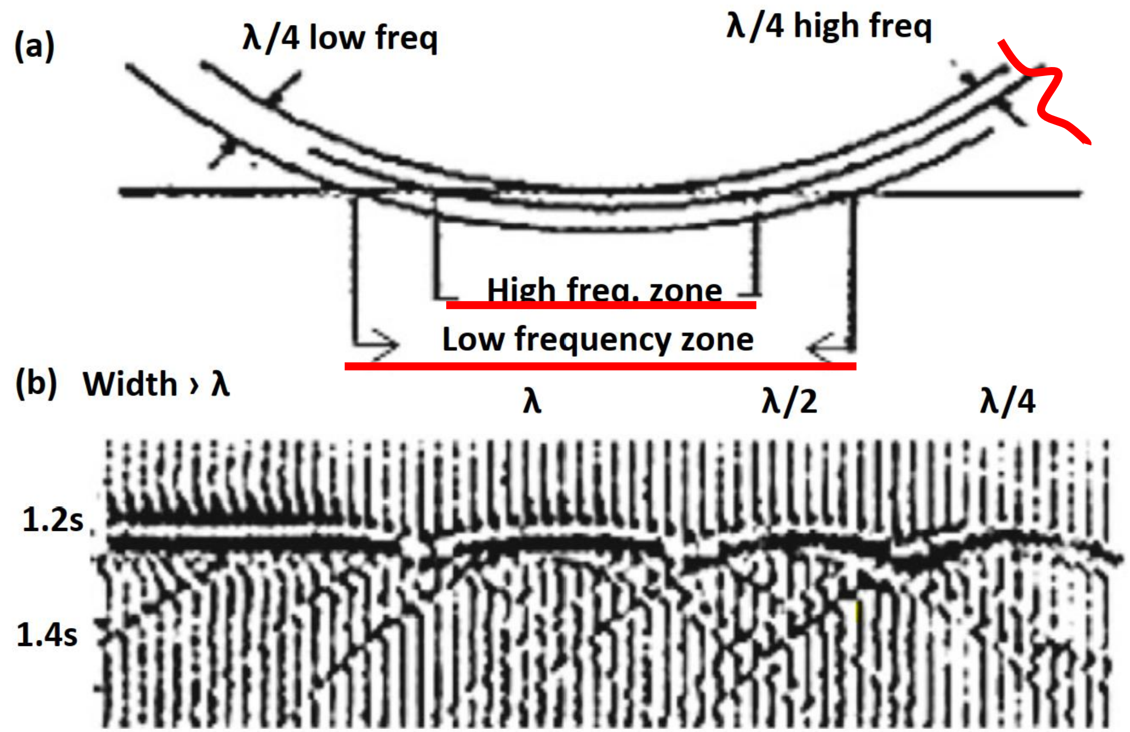

Fig. 5 Schematic illustrating phenomenon of reflection and the Fresnel's zone. (**a**) Spherical wave front incident on plane surface forms contact zones of different widths for each of the frequencies in the bandwidth. However, the contact area for the dominant frequency mainly influences creating reflection events and is known as the (first) Fresnel zone and is a measure of lateral resolution. Smaller the zone-width better is the resolution. The width of Fresnel zone at a depth is dependent on frequency, being larger for low frequency than for high frequency. (**b**) Synthetic reflection events computed with variable source wavelength. Notice the start of deterioration in reflection at λ/4, which sets this as the limit of spatial resolution (after Meckel and Nath 1977)

$$R \approx \sqrt{\lambda \cdot \frac{z}{2}}$$

Migración

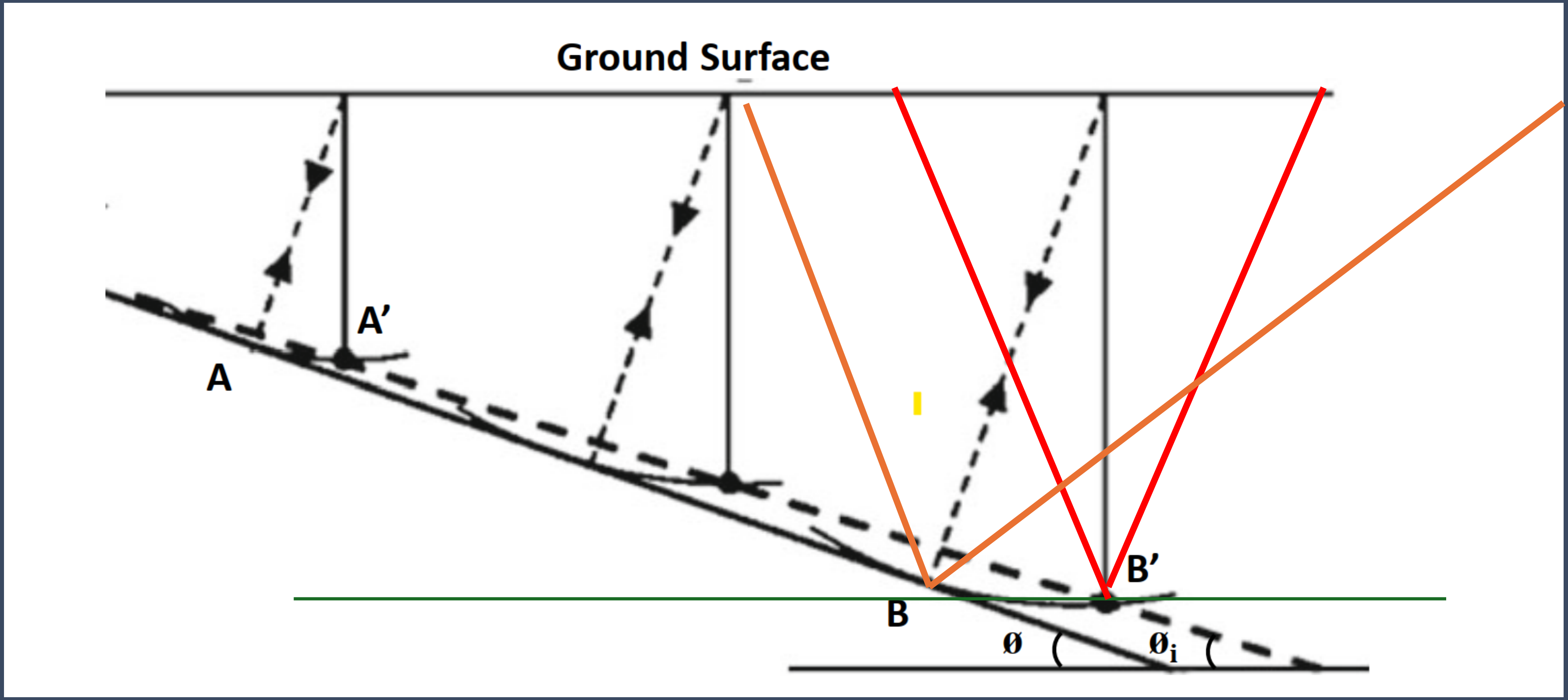

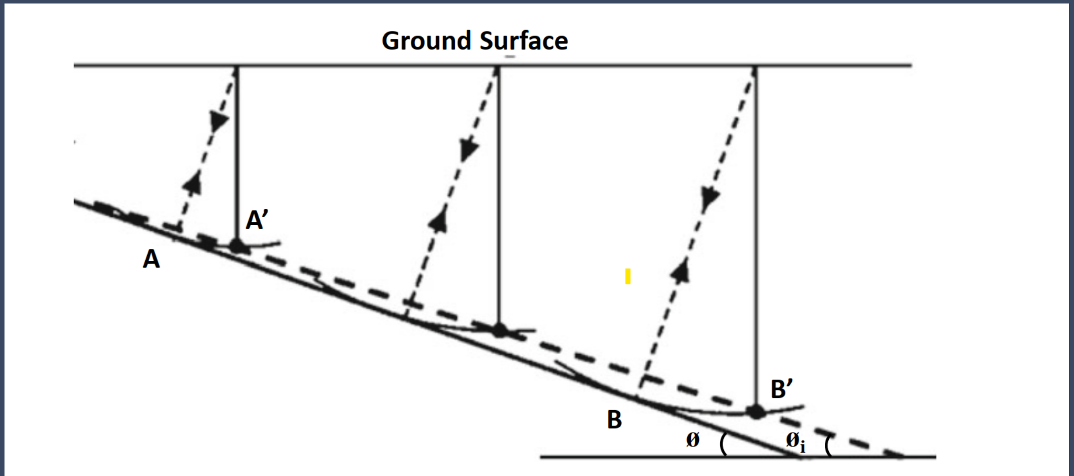
Ground Surface
A'
A
B'
B
ø
$ø_i$

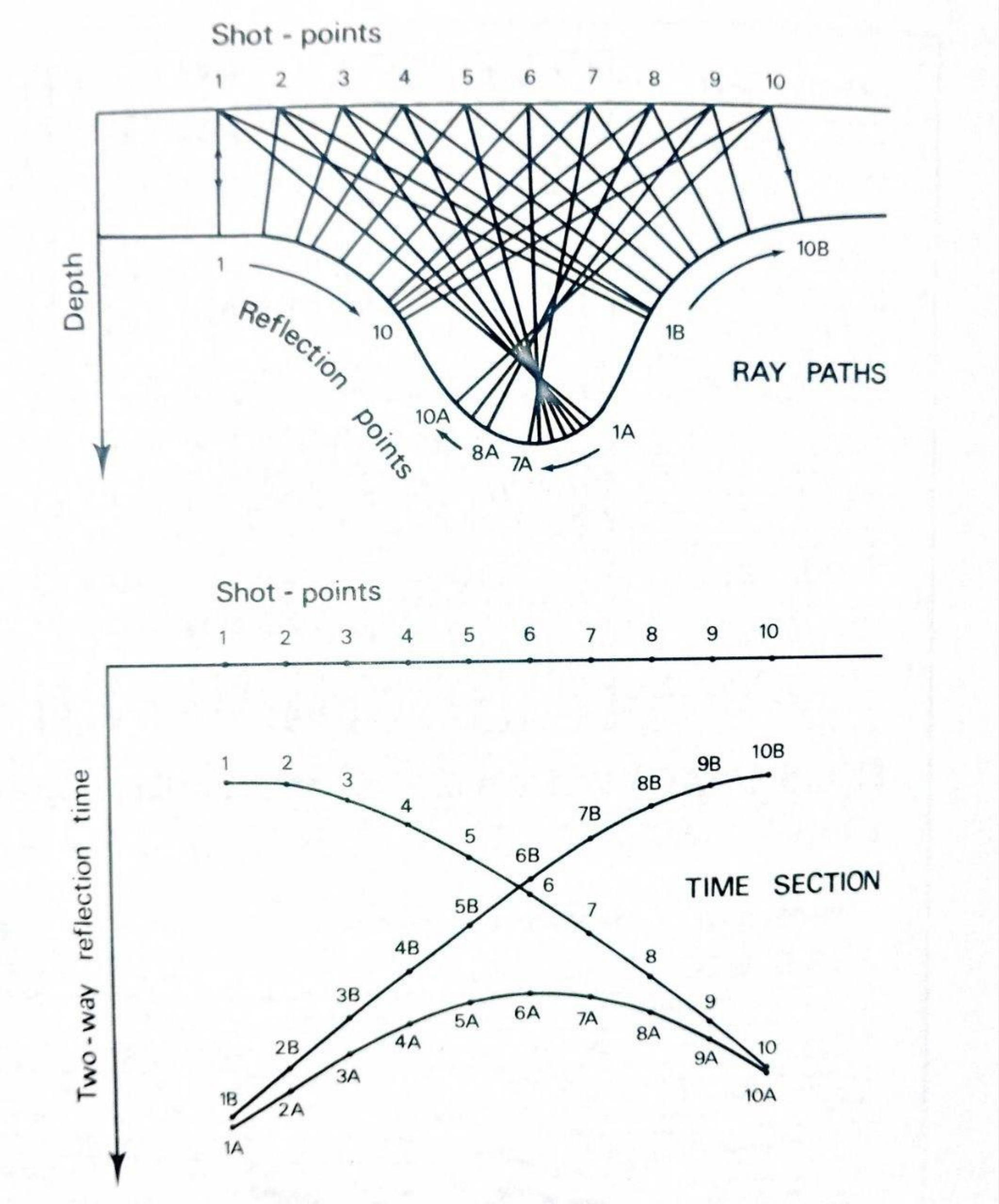
Shot - points
1 2 3 4 5 6 7 8 9 10
Depth
1
10
Reflection points
10A
8A
7A
1A
1B
10B
RAY PATHS
Shot - points
1 2 3 4 5 6 7 8 9 10
Two-way reflection time
TIME SECTION
1B 2B 3B 4B 5B 6B 7B 8B 9B 10B
1A 2A 3A 4A 5A 6A 7A 8A 9A 10A

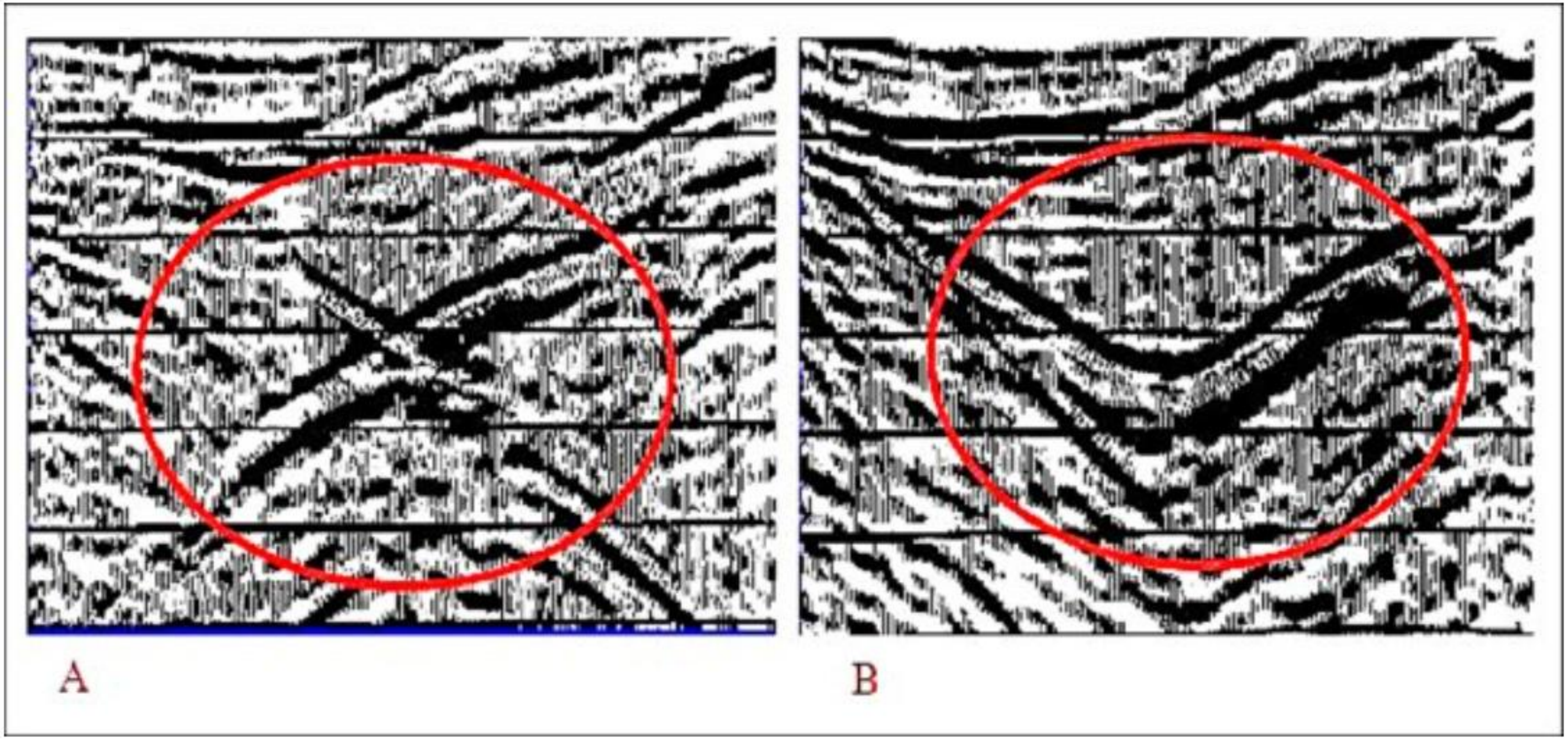
A
B

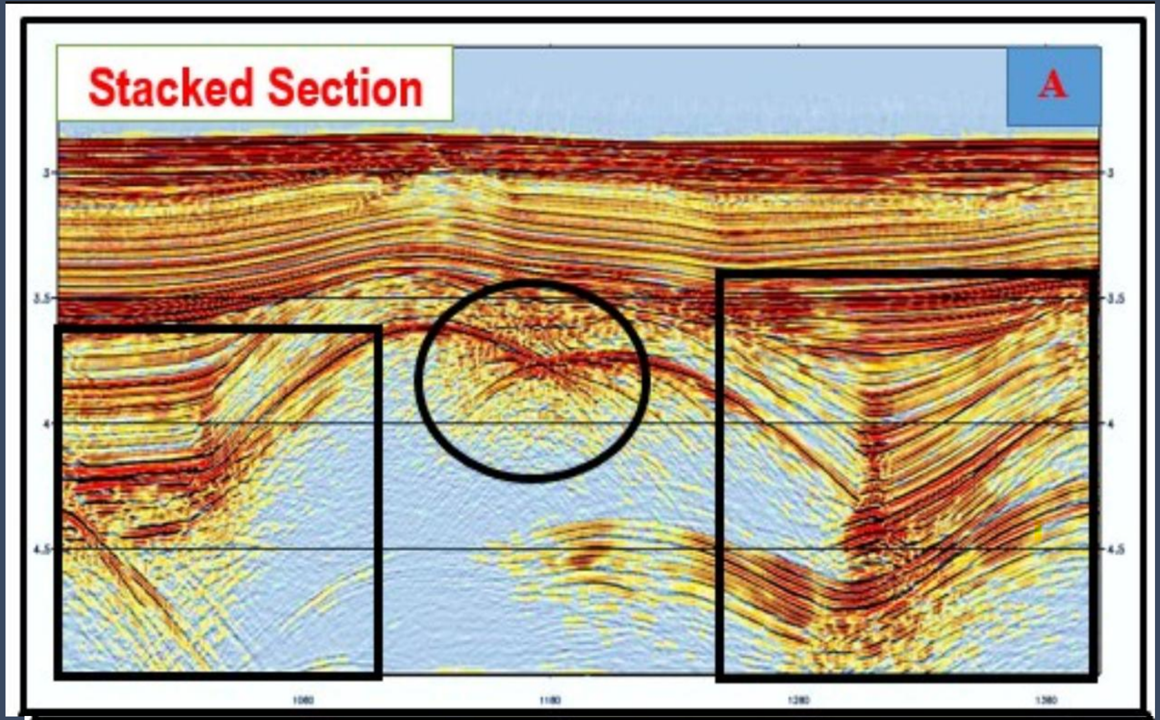
Stacked Section
A

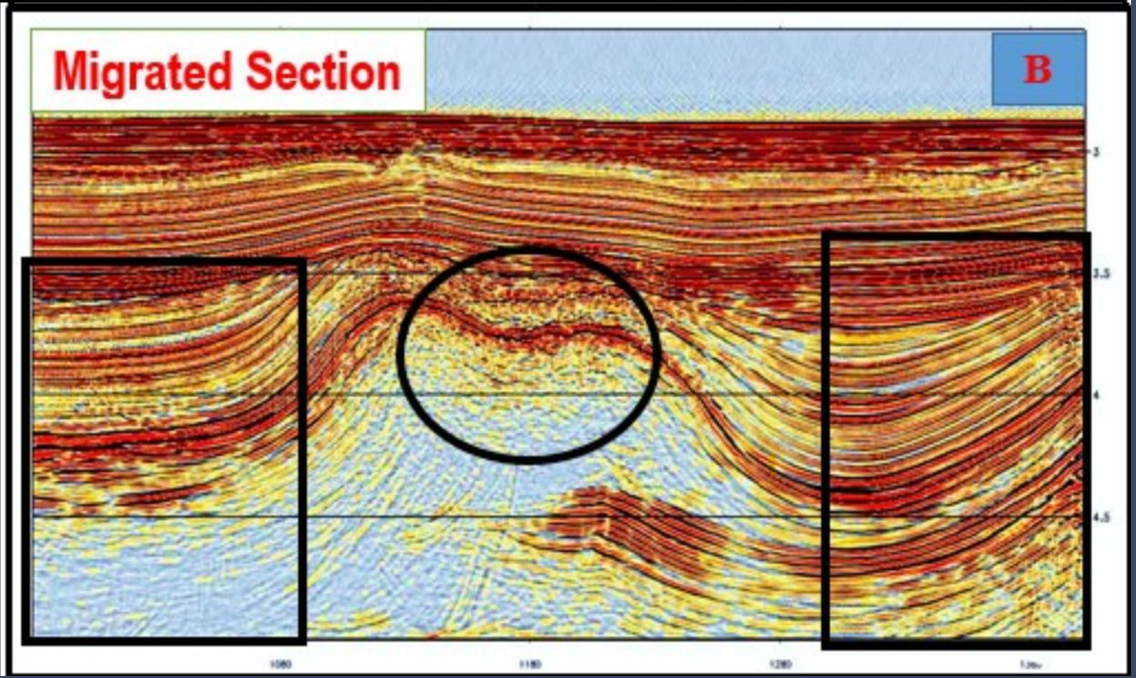
Migrated Section
B

Flujo de Trabajo 1/2

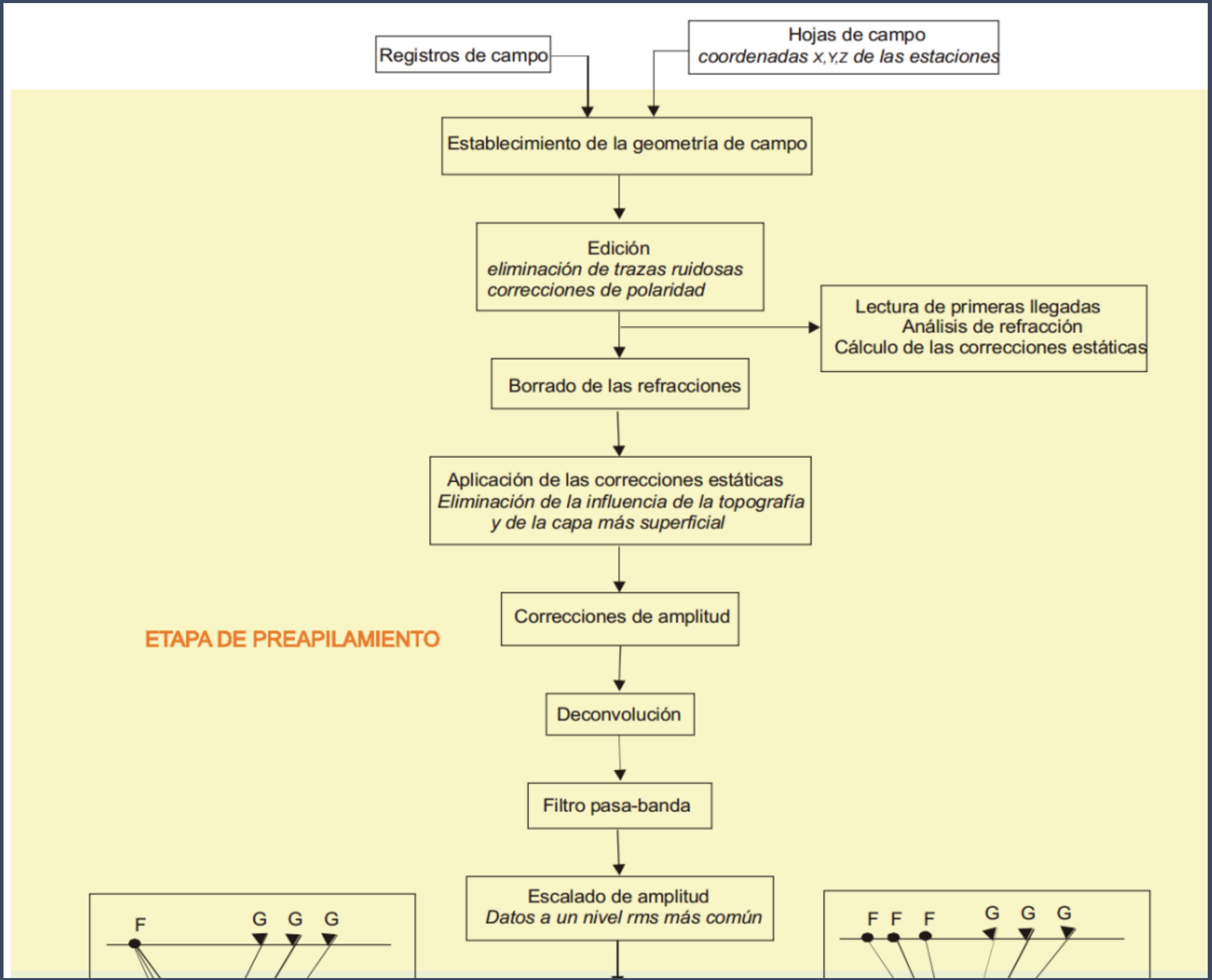

Flujo de Trabajo 2/2

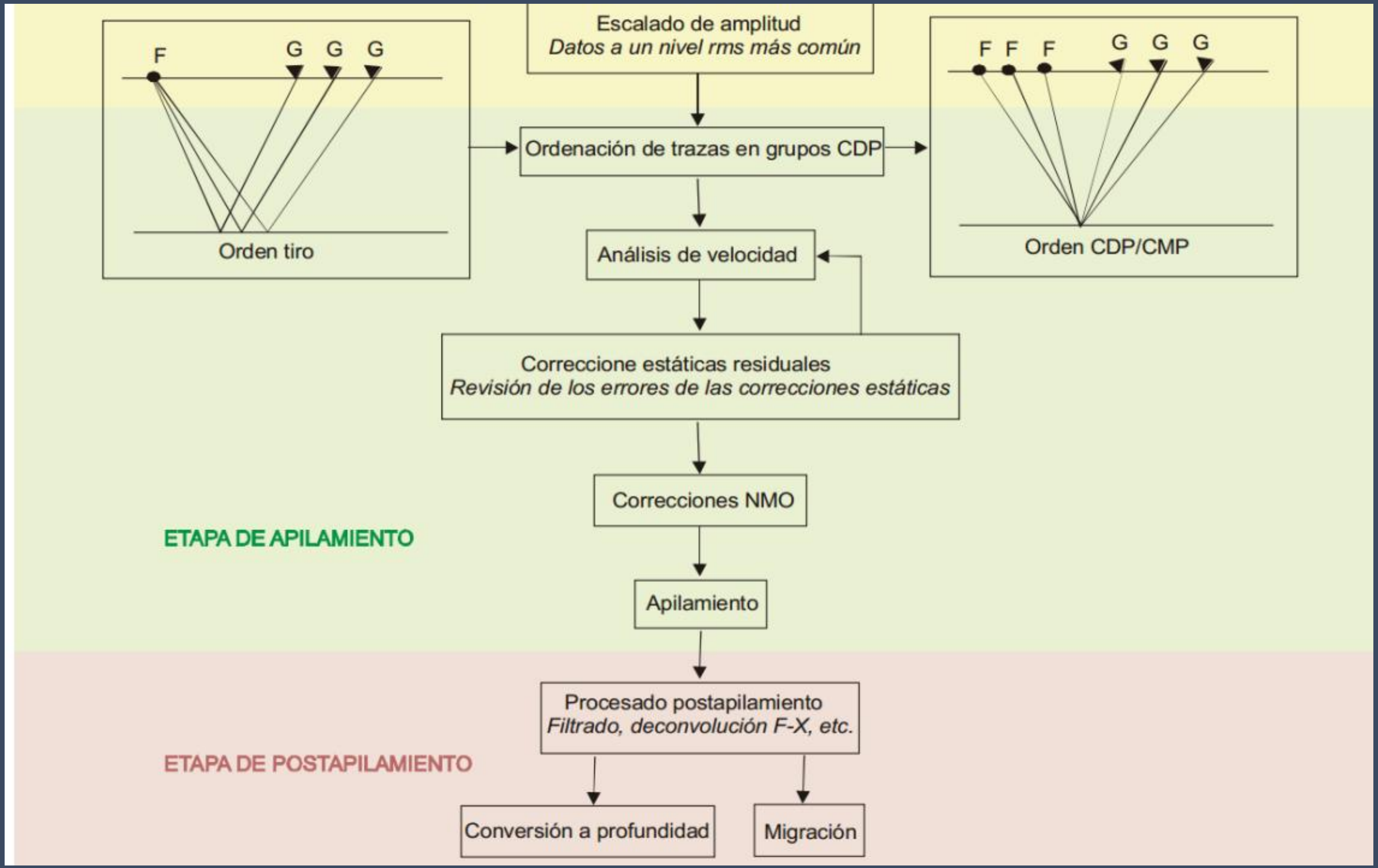

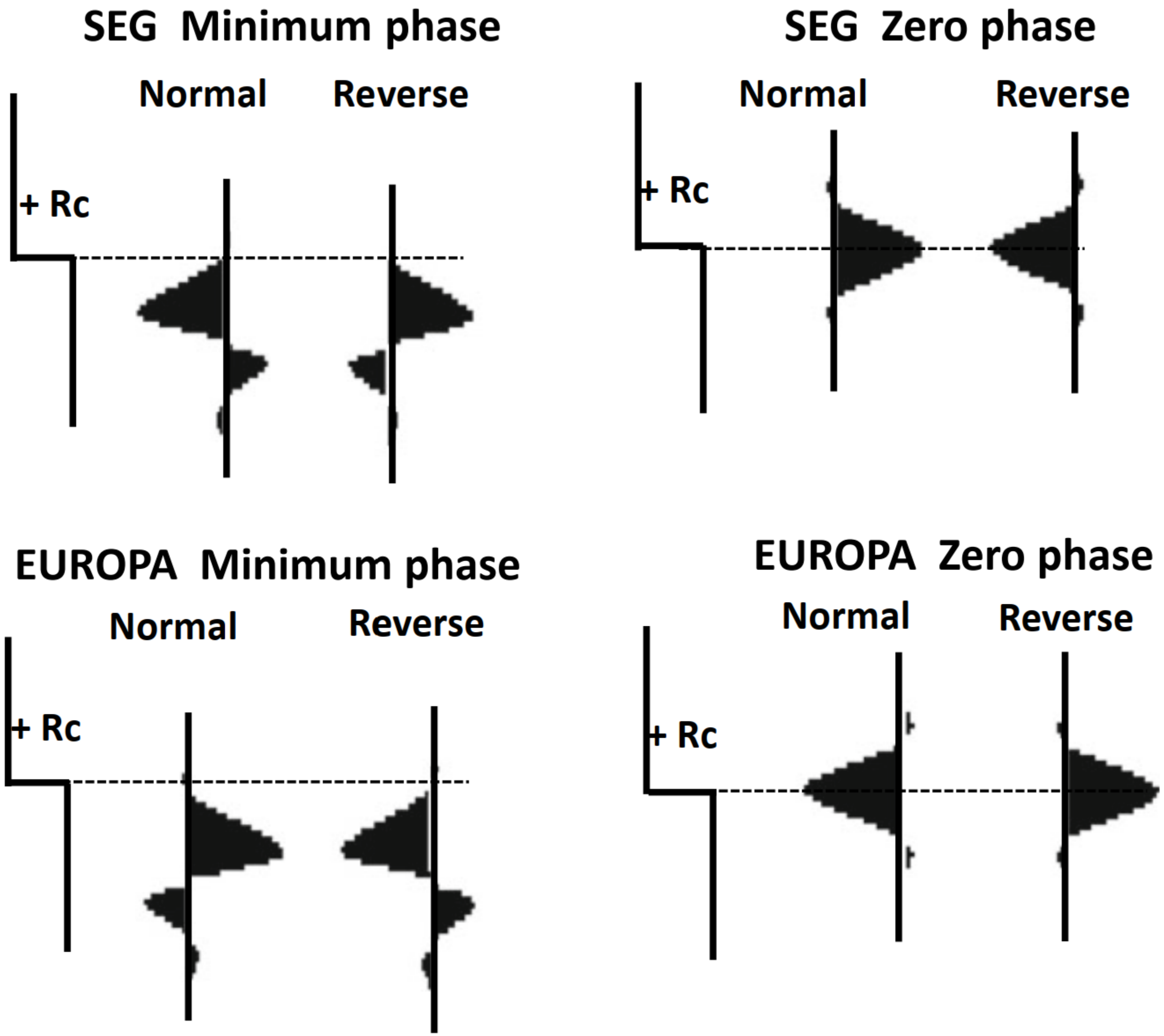

Fig. 12 Display of different polarity conventions for minimum and zero phase source wavelets in SEG and Europa, Normal and Reverse. Note the opposite polarity conventions for minimum and zero phase wavelets in both SEG and Europa. The Europa convention is opposite to corresponding SEG convention

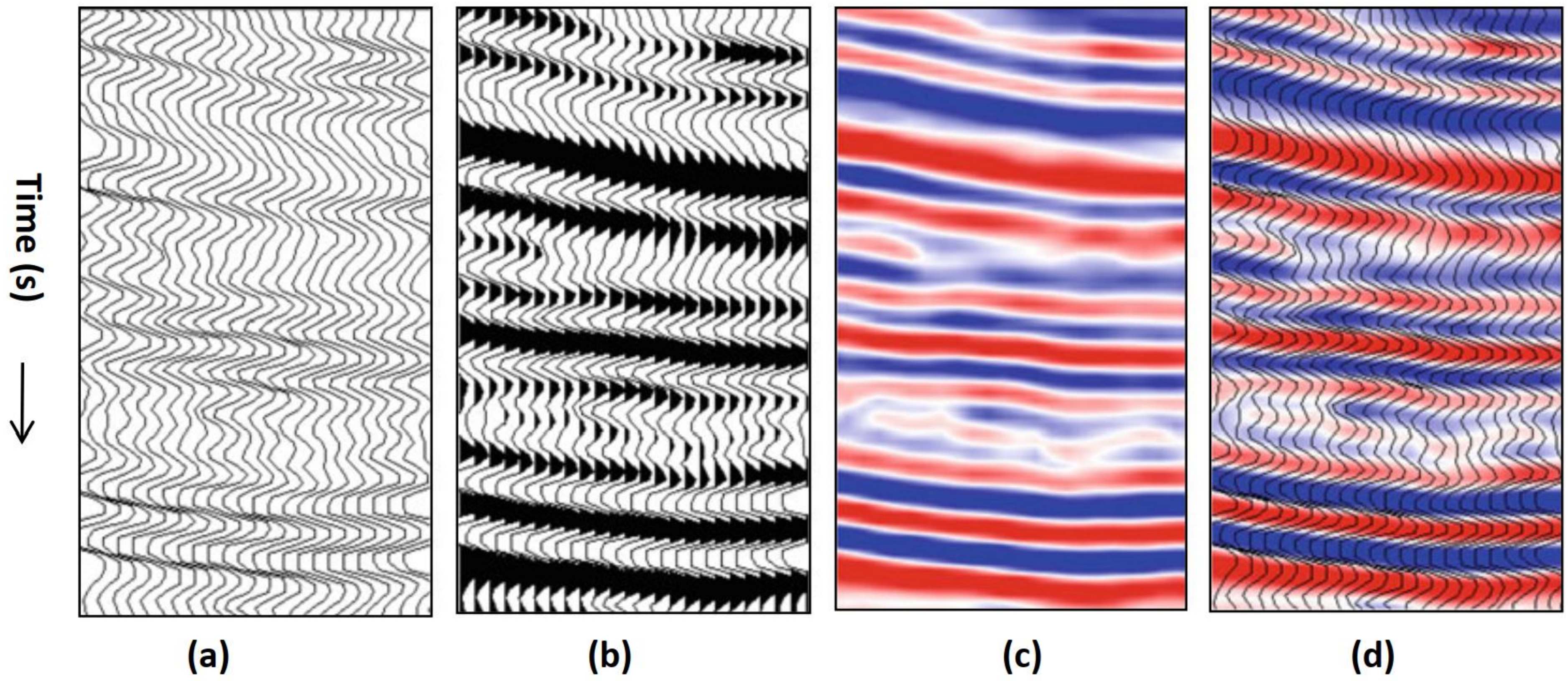

Fig. 16 Seismic segments showing types of display modes. (**a**) wiggle, (**b**) wiggle and variable area, (**c**) variable density, (**d**) combination of wiggle and variable density. Note the lateral changes in wave form seen clearly in wiggle and variable area mode (**b**) but not so clear in (**c**). Lateral variability in wave forms provide valuable geologic information

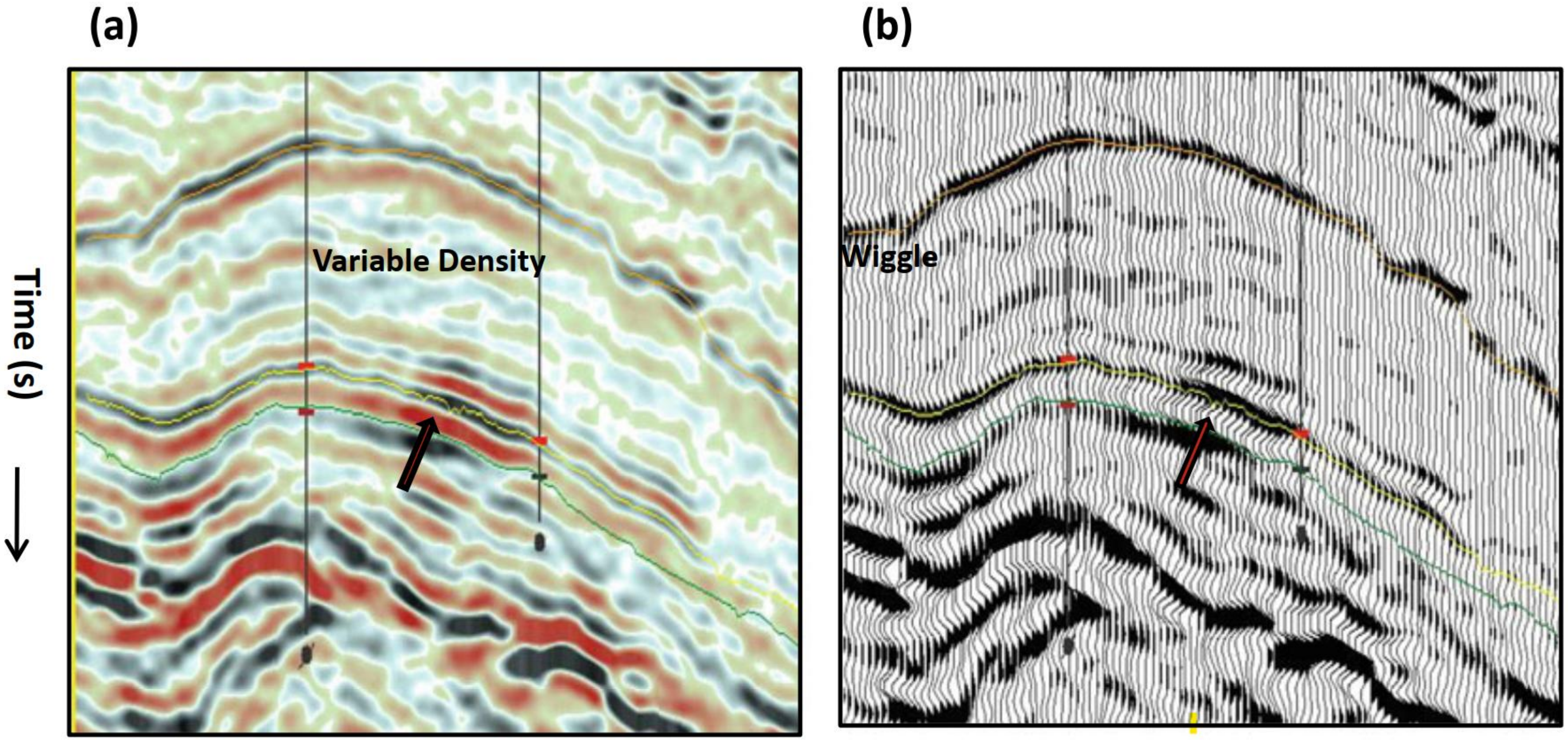

Fig. 17 Seismic image in display modes showing comparison of (**a**) variable density and (**b**) Wiggle with variable area modes. Reflection standouts and continuity are seen better in the variable density, but does not show the changes in wave form and misses the important geologic information they carry. Wiggle and VA mode shows clearly the variations (the trough marked by arrow) and help proper correlation based on reflection character and also offer geologic information from the lateral change of wave forms (image: courtesy, Hardy Energy, India)

Sísmica 3D

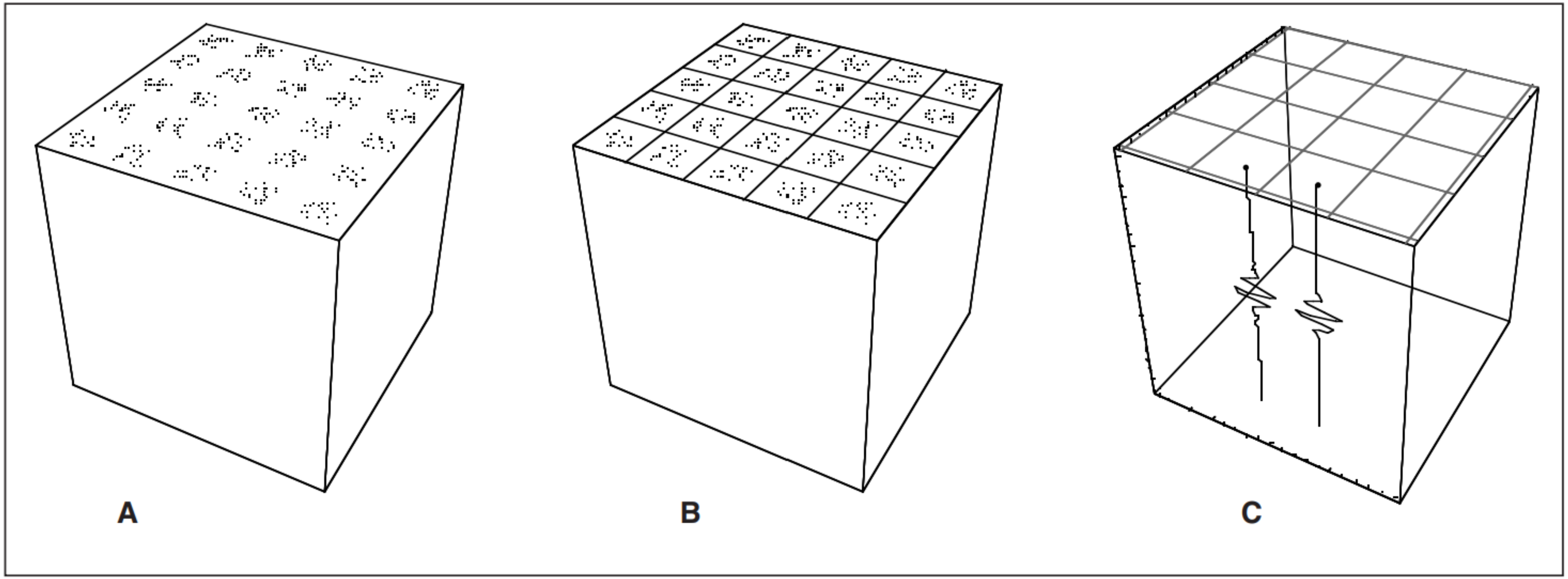

Figure 12–4. From Liner, 1999; courtesy PennWell.

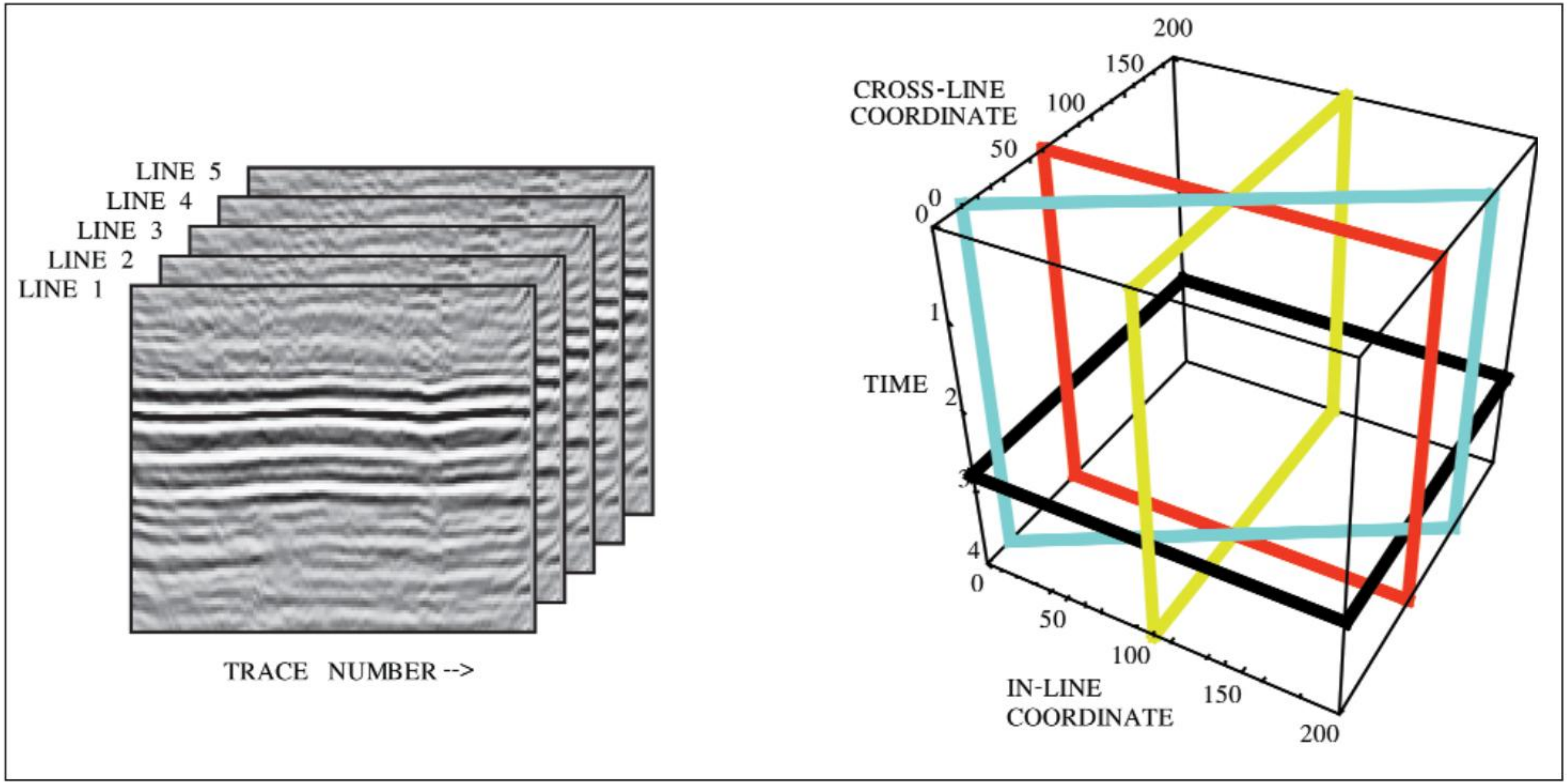

Figure 12–5. From Liner, 1999; courtesy PennWell.

Sísmica de Pozo VSP (Vertical Seismic Profile)

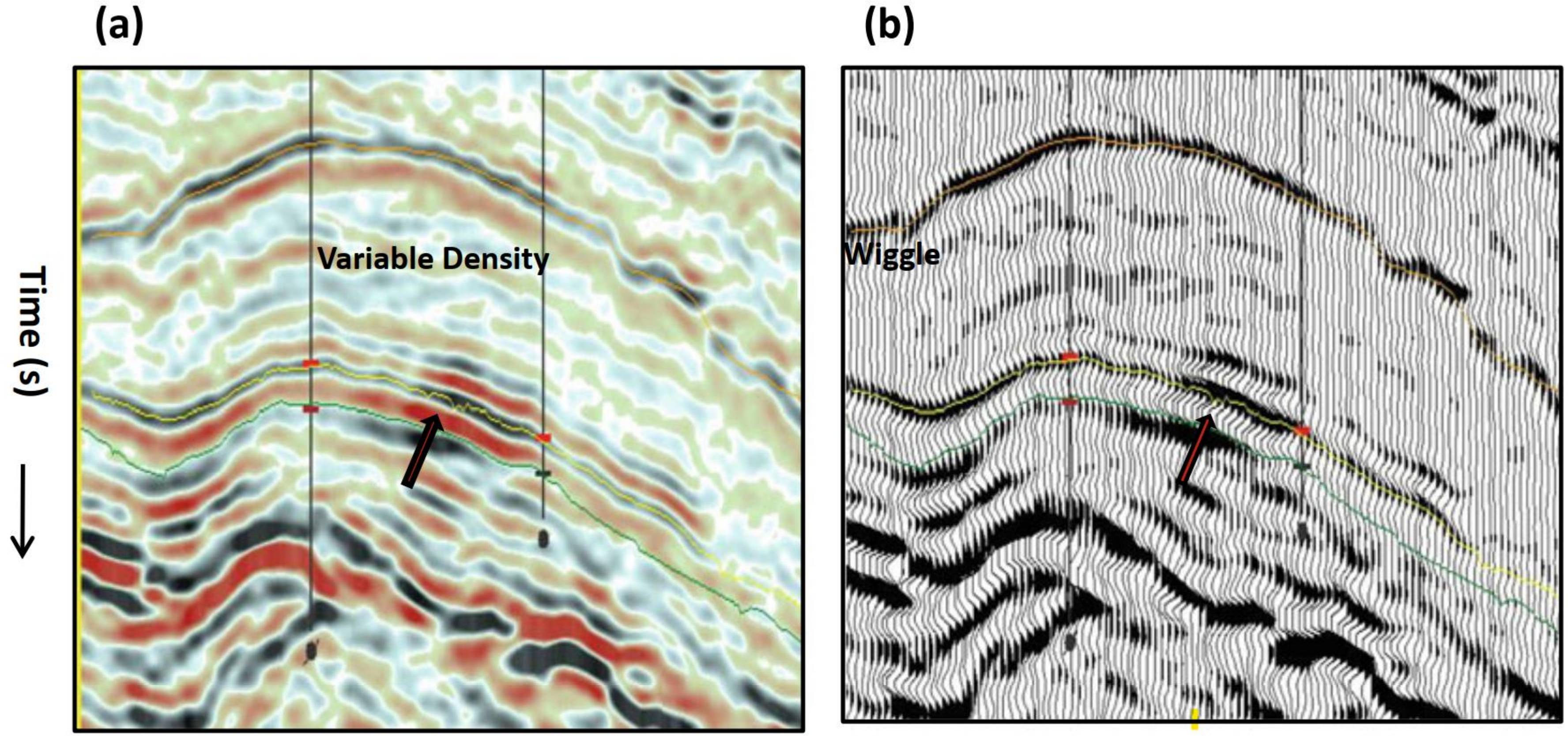

Fig. 17 Seismic image in display modes showing comparison of (**a**) variable density and (**b**) Wiggle with variable area modes. Reflection standouts and continuity are seen better in the variable density, but does not show the changes in wave form and misses the important geologic information they carry. Wiggle and VA mode shows clearly the variations (the trough marked by arrow) and help proper correlation based on reflection character and also offer geologic information from the lateral change of wave forms (image: courtesy, Hardy Energy, India)

Sismograma sintético

$$CR = \frac{Z_2 - Z_1}{Z_2 + Z\_1}$$

$$Z_i = \rho_i \cdot v_i$$

Perfil de densidad

Perfil Sónico

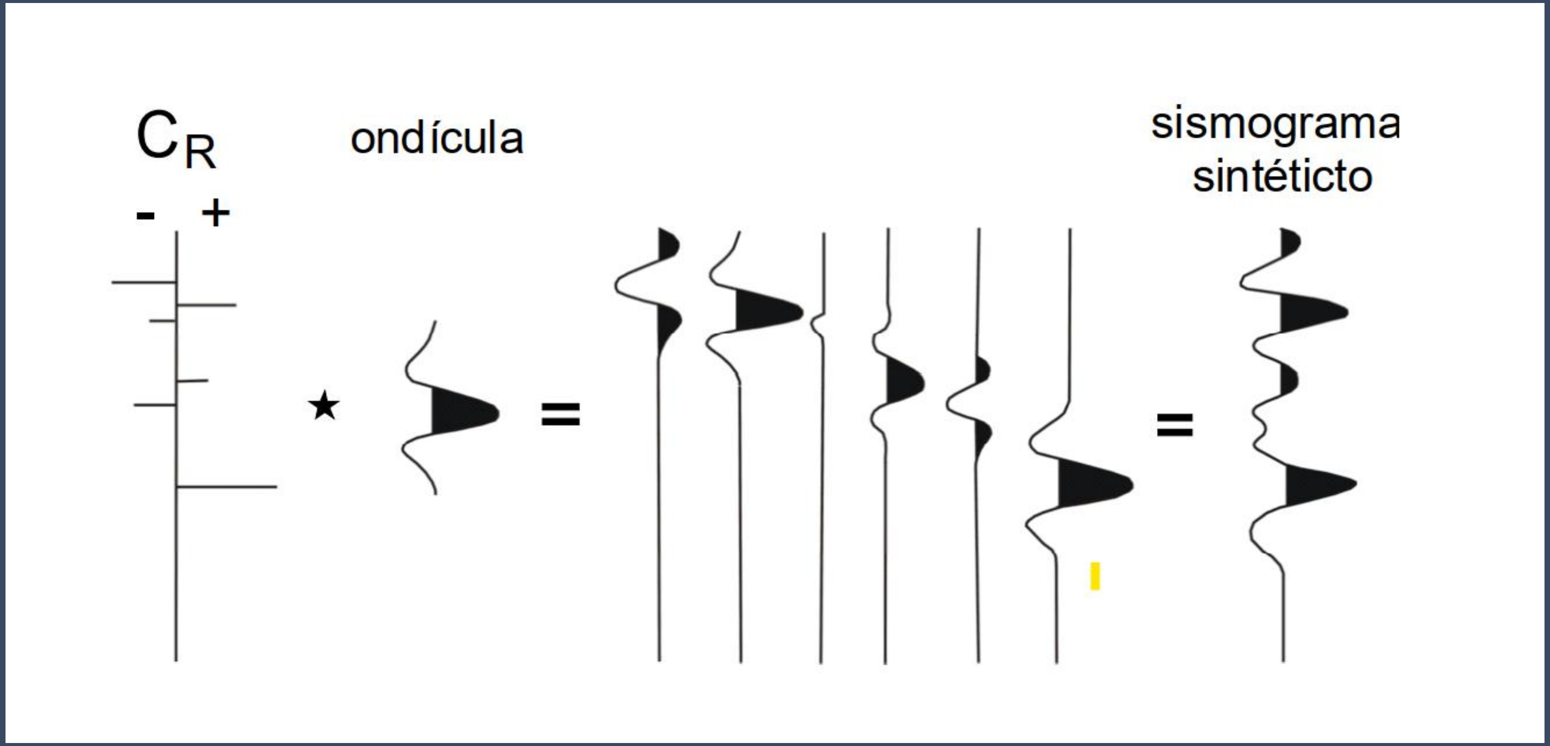

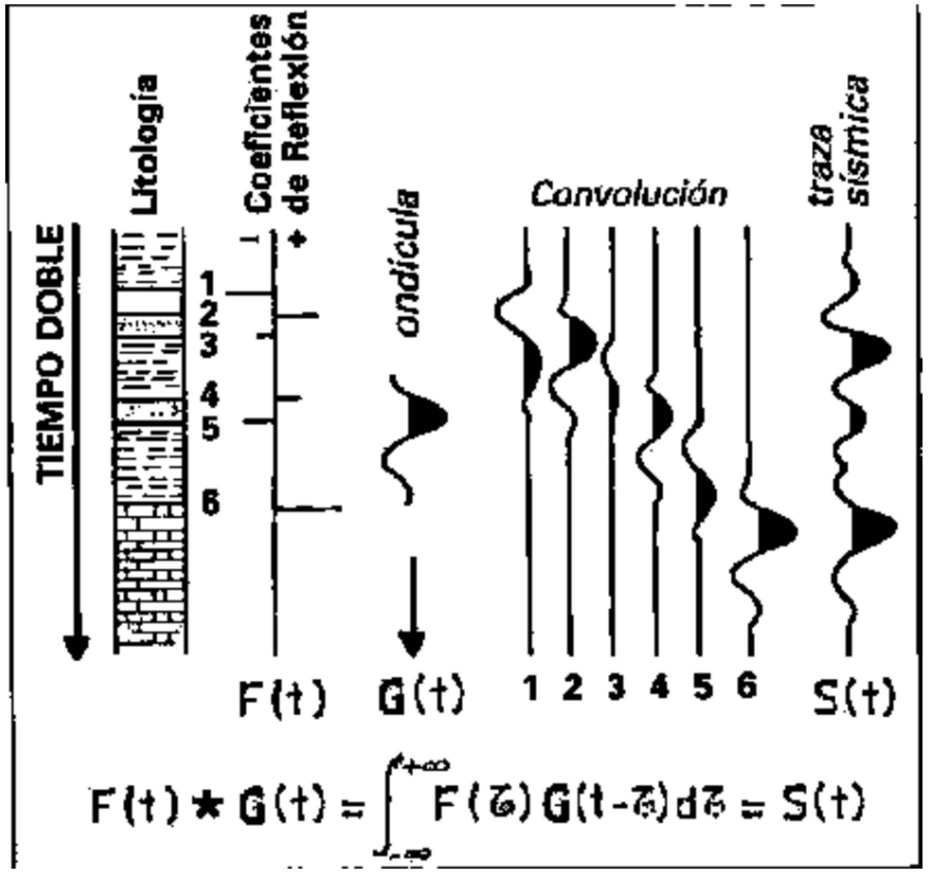

Figura 14: Operación matemática de convolución; modelo de traza sísmica, (Chelotti *et al*, 2010).

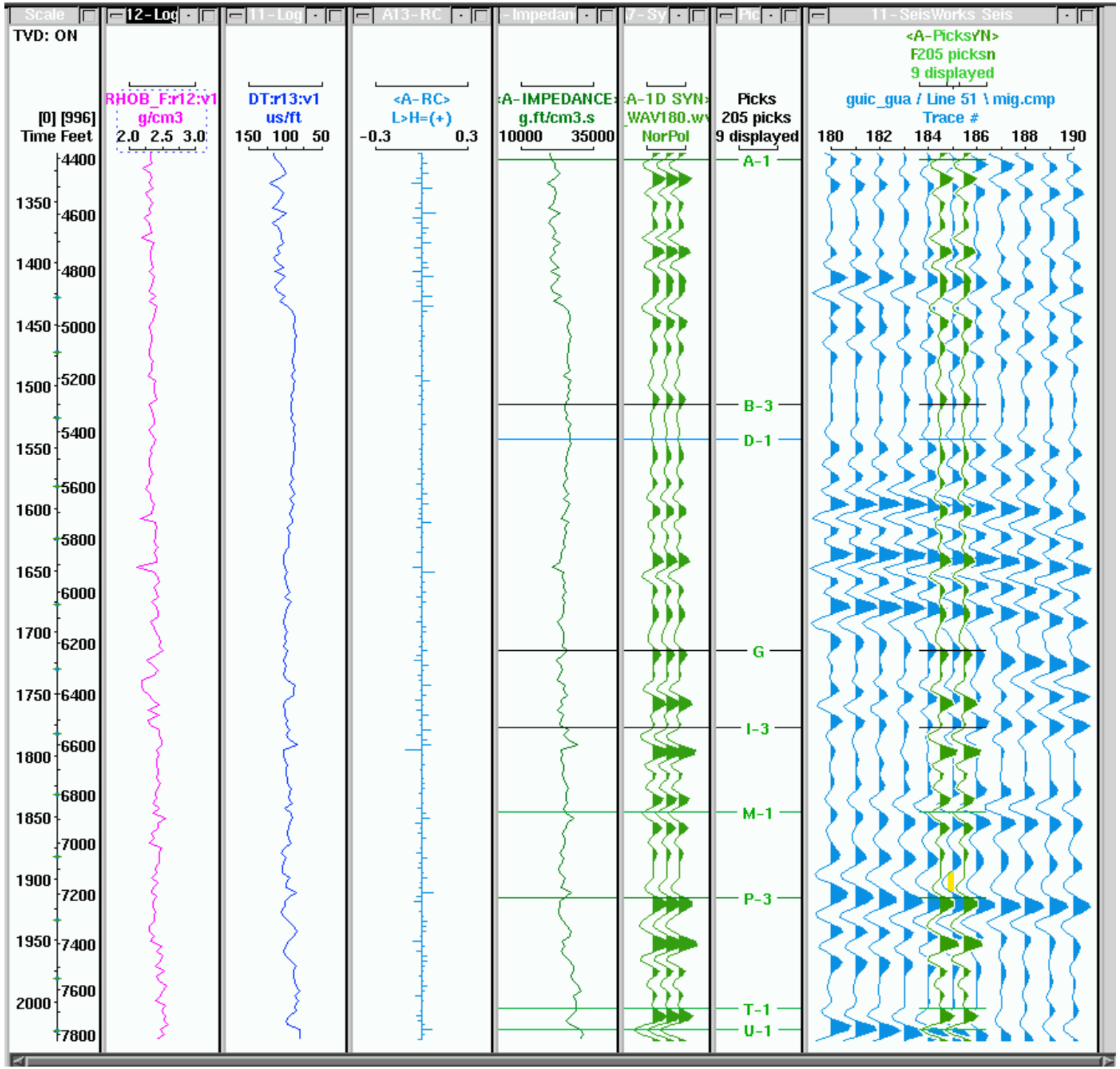

TVD: ON
[0] [996]
Time Feet
RHOB_F:r12:v1
g/cm3
2.0 2.5 3.0
DT:r13:v1
us/ft
150 100 50
<A-RC>
L>H=(+)
-0.3 0.3
A-IMPEDANCE
g.ft/cm3.s
10000 35000
A-1D SYN
WAV180.w
NorPol
Picks
205 picks
9 displayed
<A-PicksYN>
F205 picksn
9 displayed
guic_gua / Line 51 \ mig.cmp
Trace #
180 182 184 186 188 190
A-1
B-3
D-1
G
I-3
M-1
P-3
T-1
U-1
1350
1400
1450
1500
1550
1600
1650
1700
1750
1800
1850
1900
1950
2000
4400
4600
4800
5000
5200
5400
5600
5800
6000
6200
6400
6600
6800
7000
7200
7400
7600
7800

VSP

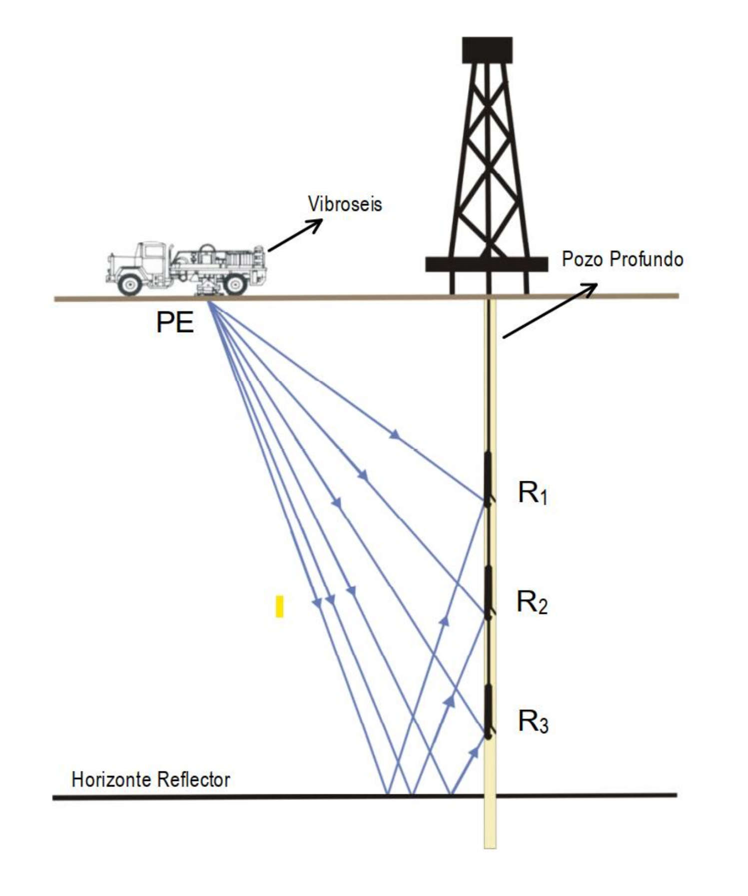
Vibroseis
Pozo Profundo
PE
R1
R2
R3
Horizonte Reflector

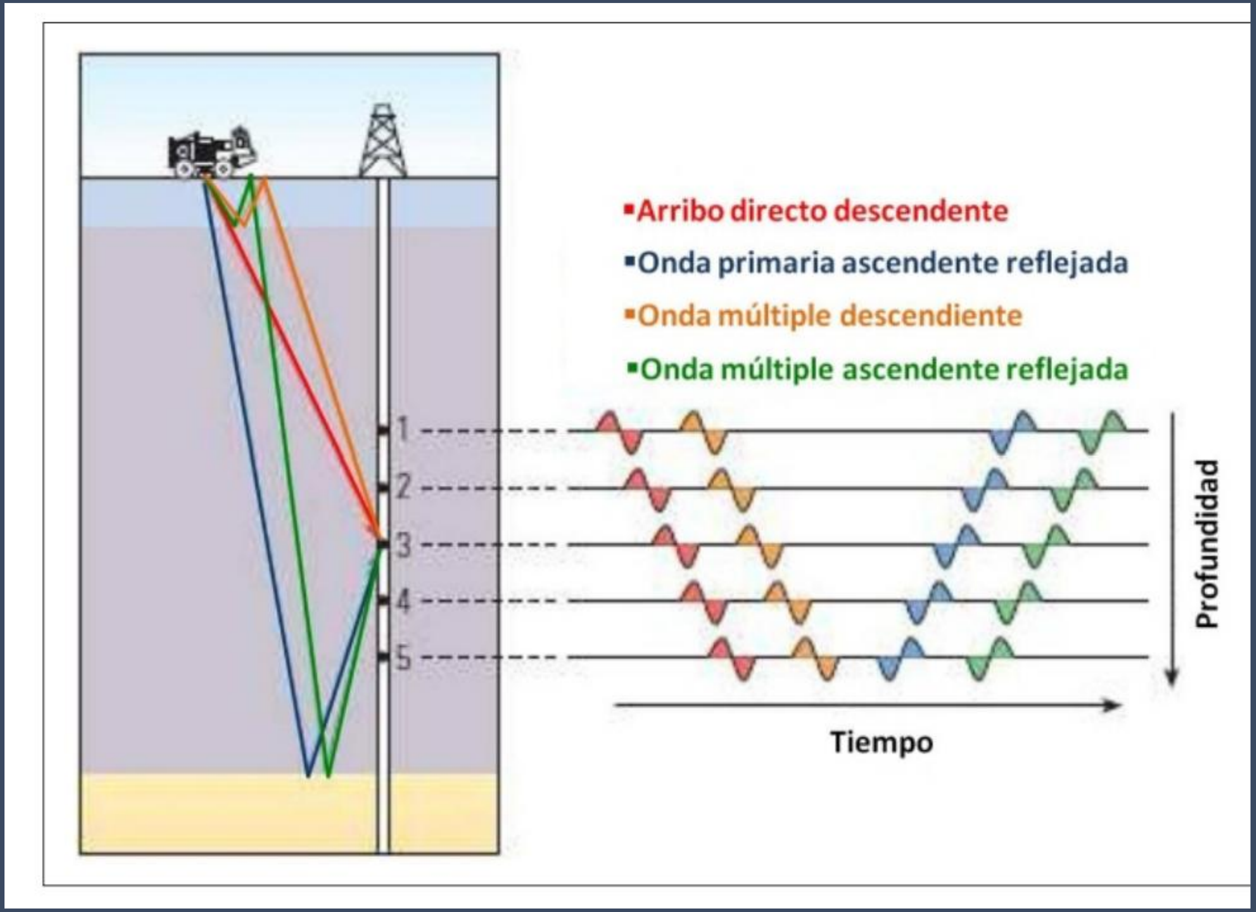
▪Arribo directo descendente
▪Onda primaria ascendente reflejada
▪Onda múltiple descendiente
▪Onda múltiple ascendente reflejada
1
2
3
4
5
Profundidad
Tiempo

- ***Checkshot***
- ***VSP Cero Offset (ZVSP)***
- ***VSP Offset (OVSP)***
- ***VSP Walkaway***

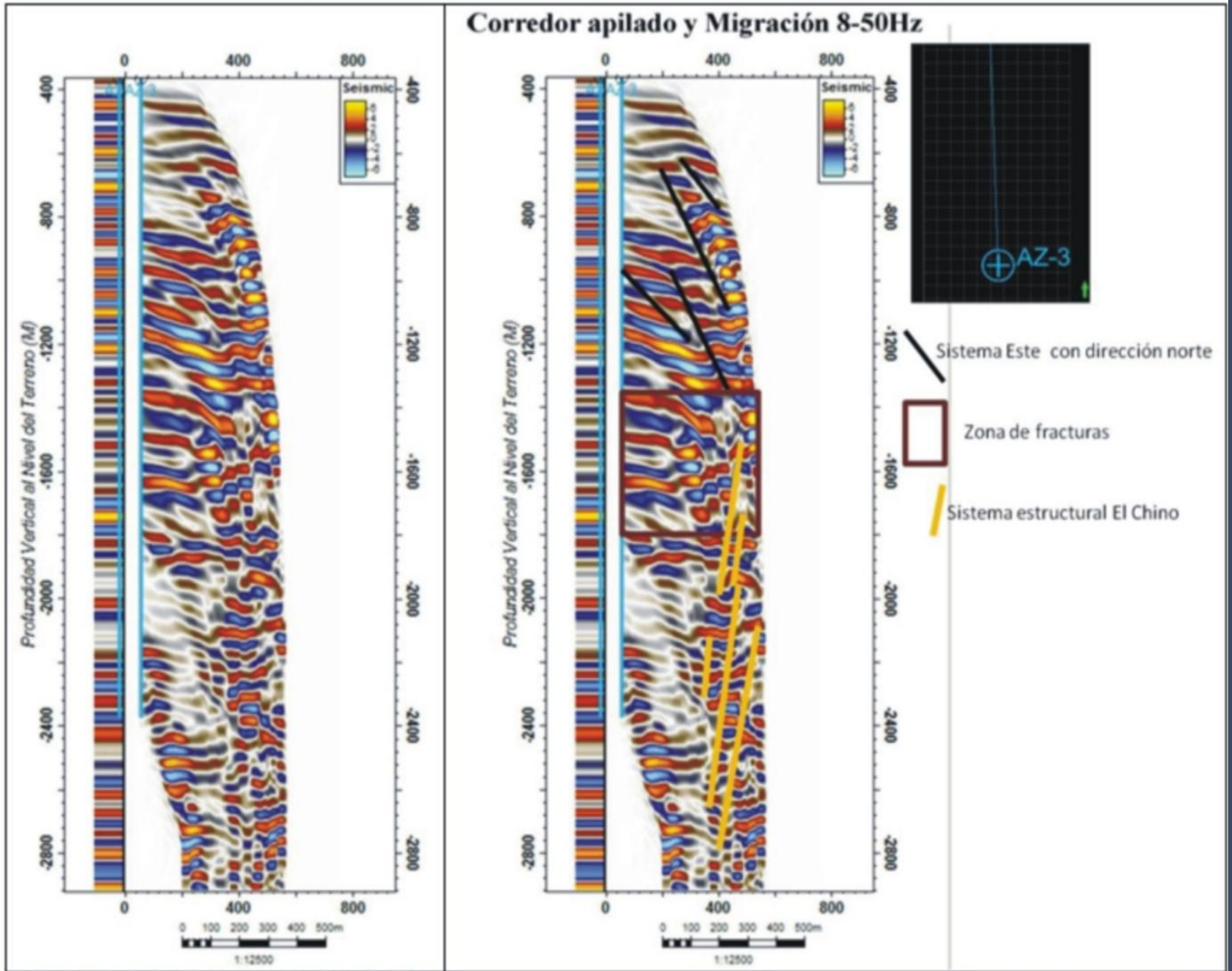

Figura 4.4.1.-Imagen 1D (ZVSP) y 2D (OVSP) (Tomada de Parga-

Figura 4.4.2.-Interpretación del registro OVSP.

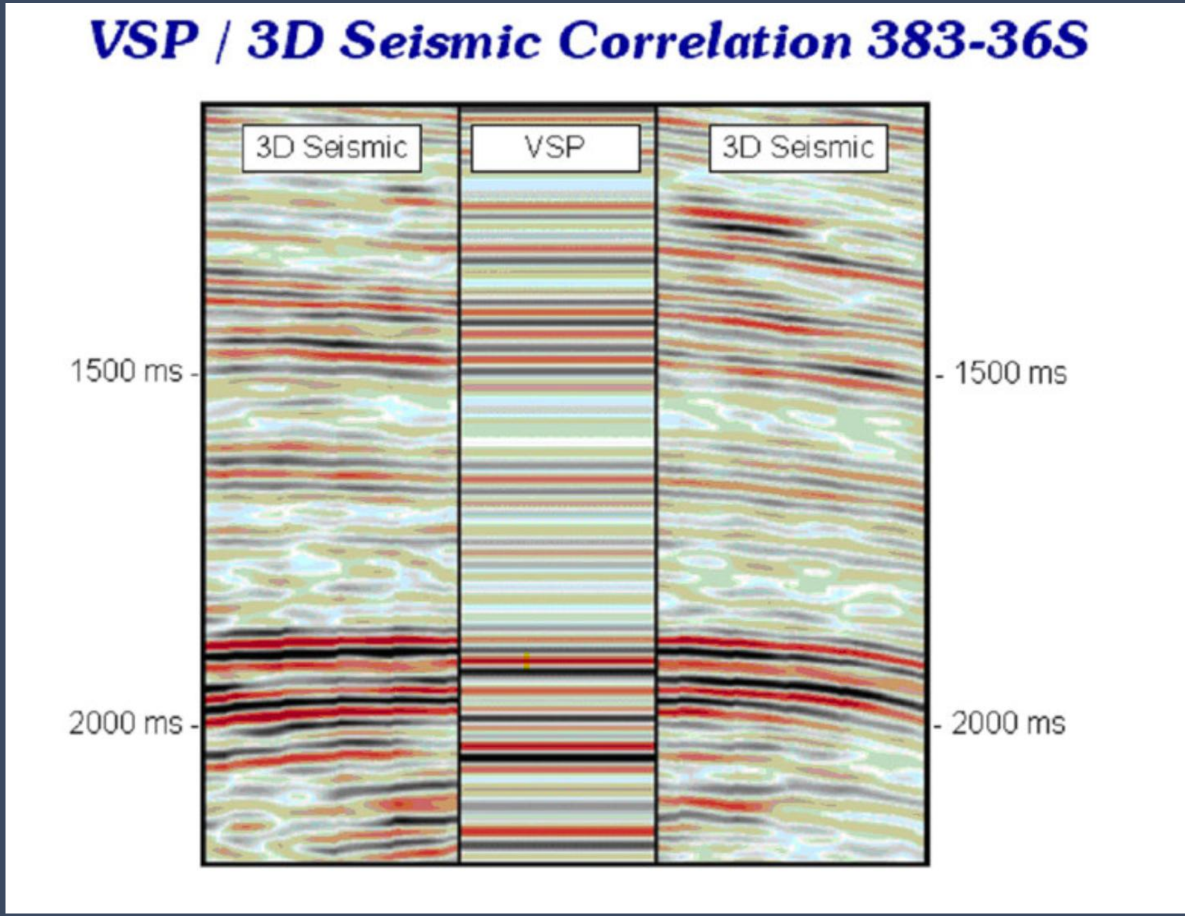
VSP / 3D Seismic Correlation 383-36S
3D Seismic
VSP
3D Seismic
1500 ms
1500 ms
2000 ms
2000 ms

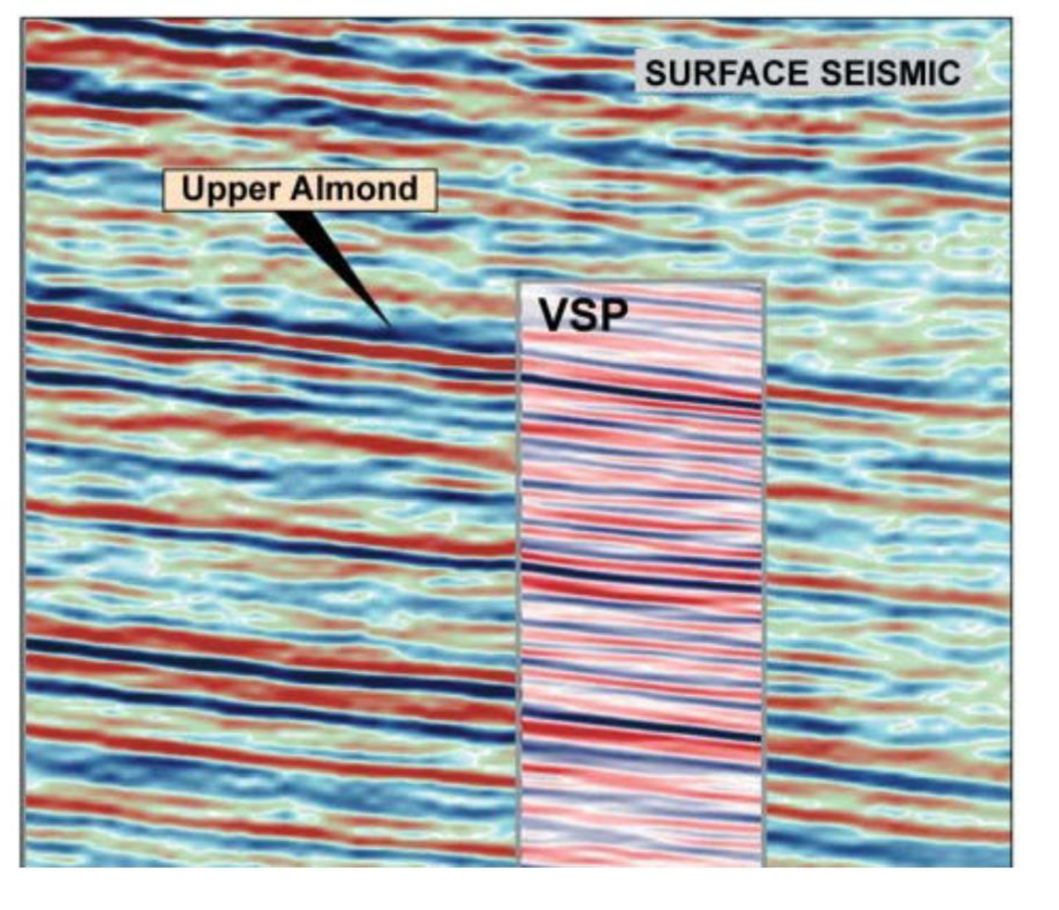
SURFACE SEISMIC
Upper Almond
VSP